

F. Giorgi · X. Bi · J. S. Pal

## Mean, interannual variability and trends in a regional climate change experiment over Europe. I. Present-day climate (1961–1990)

Received: 12 August 2003 / Accepted: 2 February 2004 / Published online: 12 May 2004  
© Springer-Verlag 2004

**Abstract** We present an analysis of a multidecadal simulation of present-day climate (1961–1990) over Europe with the regional climate model RegCM nested within the global atmospheric model HadAMH. Climatic means, interannual variability and trends are examined, with focus on surface air temperature and precipitation. The RegCM driven by HadAMH fields is able to reproduce the basic features of the observed mean surface climate over Europe, its seasonal evolution and the regional detail due to topographic forcing. Surface air temperature biases are mostly less than 1–2 °C and precipitation biases mostly within 10–20%. The RegCM has more intense vertical transport of temperature and water vapor than HadAMH, which results in lower surface air temperatures and greater precipitation than found in the HadAMH simulation. In some cases this is in the direction of greater agreement with observations, while in others it is in the opposite direction. The simulation shows a tendency to overestimate interannual variability of temperature and precipitation compared to observations, particularly during summer and over the Mediterranean regions. It is shown that in DJF, MAM and SON the RegCM interannual variability is primarily determined by the boundary forcing from HadAMH, while in JJA the internal model physics and resolution effects dominate over many subregions of the domain, and the RegCM has higher interannual variability than HadAMH. The precipitation trends simulated by the nested modeling system for the period 1961–1990 capture some features of the observed trends, in particular the cold season drying over the Mediterranean regions. Ensembles of simulations are, however, needed for a more robust assessment of the model's capability to simulate climatic trends. Overall, this simulation is of good quality compared

with previous nested RegCM experiments and will constitute the basis for the generation of climate change scenarios over the European region to be reported in future work.

### 1 Introduction

Nested regional climate models (RCMs) have been increasingly used over the last decade to produce climate change information at the regional scale (e.g., Giorgi and Mearns 1991, 1999; McGregor 1997). In particular, a number of regional climate experiments have been completed for the European region to assess the possible changes associated with increased concentrations of greenhouse gases (GHG) (Giorgi et al. 1992, 1997; Jones et al. 1995, 1997; Christensen et al. 1997; Christensen et al. 1998; Rotach et al. 1997; Machenauer et al. 1998; Räisänen et al. 2001; Räisänen and Joelsson 2001; Christensen and Christensen 2003). These experiments used a range of simulation lengths (5 to 30 years), horizontal grid intervals (20–70 km) and model configurations, and provided valuable information on some mechanisms of fine scale climate change over Europe and on the systematic biases of regional models over this region.

One of the issues that have been raised in the Third Assessment Report of the Intergovernmental Panel on Climate Change (IPCC 2001) is the lack of coordinated RCM experiments necessary to provide a comprehensive view of regional climate changes (Giorgi et al. 2001). This problem has also hindered a robust evaluation of the uncertainties related to the projection of regional climate changes. Partially to address these issues, the project PRUDENCE (Prediction of Regional scenarios and Uncertainties for Defining European Climate change risks and Effects, Christensen et al. 2002) has been recently established aimed at improving our understanding of regional climate change and related

F. Giorgi (✉) · X. Bi · J. S. Pal  
Abdus Salam International Centre  
for Theoretical Physics, Trieste, Italy  
E-mail: giorgi@ictp.trieste.it

uncertainties over the European region. The project is based on a series of coordinated simulations with different RCMs for various GHG and aerosol emission scenarios, where all RCMs use comparable domain, horizontal resolution, simulation period and lateral boundary forcing fields.

As part of the PRUDENCE project, we completed three multi-decadal simulations over Europe with the regional climate model RegCM (Giorgi et al. 1993a,b; Giorgi and Mearns 1999) nested within the Hadley Centre global atmospheric model HadAMH (Pope et al. 2000). The simulations cover a present day 30-year climate period (1961–1990) and a 30-year future climate period (2071–2100) for the A2 and B2 IPCC emission scenarios (IPCC 2000). The purpose of these simulations is to analyze the regional climate change signal over the European region as affected by the local high-resolution forcings, the emission scenarios and, in coordination with the other PRUDENCE model experiments, the different modeling systems.

The first step towards a better understanding of the climate change signal is an analysis of the present-day climate simulation (hereafter referred to as “reference” simulation), which allows the identification and possibly the physical interpretation of systematic model errors. Such an analysis is thus presented here while the climate scenario experiments are examined in a companion paper in preparation.

In our study we assess a number of measures of model performance. We begin with the climatological means and biases, which give an opportunity to identify systematic model errors and to compare the model performance with previous experiments that employed different driving global models and earlier versions of the RegCM (e.g., Marinucci and Giorgi 1992; Giorgi and Marinucci 1996b). We then analyze the model interannual variability, which is extremely important in determining the impacts of climate on many human activities (e.g., IPCC 1998). In fact, to date, despite the large number of RCM simulations documented in the literature, relatively little attention has been devoted to interannual variability, mostly because RCM simulations of sufficient length for this purpose have become available only recently.

In this regard, Giorgi and Shields (1999), Pal et al. (2000), Small et al. (1999) and Sun et al. (1999) presented evaluations of the RegCM interannual variability over the continental USA, central Asia and eastern Africa, respectively. Their simulations were driven by analyses of observations, i.e., in the “perfect boundary condition” mode, and the model showed a good performance in capturing both the sign and magnitude of the temperature and precipitation anomalies which occurred in different years over a number of subregions of the domains. Similar results from perfect boundary conditions experiments were reported by Luthi et al. (1996) and Fukutome et al. (1999) using different regional models. The performance of RCMs in reproducing the characteristics of given anomalous seasons has also been

investigated in a number of studies (e.g., Fennessy and Shukla 2000; Ji and Vernekar 1997; Cocke and LaRow 2000; Pal and Eltahir 2003; Seth and Rojas 2003; Rojas and Seth 2003)

Although even relatively short perfect boundary condition experiments can provide a measure of how a model reproduces observed climate anomalies, the evaluation of interannual variability in RCM simulations driven by forcing lateral fields from general circulation models (GCMs) is more difficult. In fact, in this latter case the model performance cannot be tested against individual events but needs to be evaluated in its statistical properties (e.g., Lal et al. 1998). Therefore, the availability of a 30-year simulation provides us with a good opportunity to examine the interannual variability in a nested RCM modeling system.

Finally, we examine and compare with observations the simulated trends throughout the 1961–1990 period. Such an analysis can provide additional insights into the ability of the nested modeling system to simulate climatic trends and changes. The availability of a single realization limits the robustness of any statements we can make in this regard, but it allows a qualitative assessment of the model reliability in simulating regional climatic trends.

The analysis presented mostly focuses on surface air temperature and precipitation over land areas within the domain, because of the importance of these fields for climate impacts, the availability of gridded observed datasets for model validation and the possibility of comparison with previous work. However, some evaluation of upper air circulation patterns is also presented in order to better assess the model behavior. After a brief description of the models and experiment design (Sect. 2) the simulation results are discussed in Sect. 3.

---

## 2 Model, experiment design and analysis strategy

### 2.1 Global atmospheric model

The global atmospheric model which provides the boundary fields for the RegCM simulations is a high resolution version of the Hadley Centre global model HadAM3, which is referred to as HadAMH. The structure of HadAM3 and its changes compared to the previous version HadAM2 are described in some detail by Pope et al. (2000). The horizontal resolution of HadAM3 is 2.5° latitude by 3.75° longitude and that of HadAMH is twice as fine, that is 1.25° latitude by 1.875° longitude. HadAMH is a hydrostatic, grid point model with hybrid vertical coordinates. A prognostic cloud scheme is used (Gregory and Morris 1996) which diagnoses cloud ice, cloud water and cloud amount from the primary model variables total moisture and liquid water potential temperature. Convection is calculated using the mass flux scheme of Gregory and Rowntree (1990) with the addition of convective downdrafts (Gregory and Allen 1991). Boundary layer processes are represented

using a simplified version of the scheme of Smith (1990, 1993), which only includes local vertical mixing (Pope et al. 2000). The radiative transfer scheme is described by Edwards and Slingo (1996) and Cusack et al. (1999) and includes the effects of a range of GHG, clouds and sulfate aerosols. Finally, the scheme of Cox et al. (1999) is used to describe land surface processes via a soil layer module, a vegetation module and a snow/soil hydrology module.

## 2.2 Regional climate model

The regional climate model used in the present work is the version of RegCM originally developed by Giorgi et al. (1993a,b) and then augmented as discussed by Giorgi and Mearns (1999) and Pal et al. (2000). The dynamical core of the RegCM is essentially equivalent to the hydrostatic version of the NCAR/Pennsylvania State University mesoscale model MM5 (Grell et al. 1994). Surface processes are represented via the Biosphere-Atmosphere Transfer Scheme (Dickinson et al. 1993) and boundary layer physics is formulated following the non-local vertical diffusion scheme of Holtslag et al. (1990). Resolvable scale precipitation is represented via the scheme of Pal et al. (2000) which includes a prognostic equation for cloud water and allows for fractional grid box cloudiness, accretion and re-evaporation of falling precipitation. Convective precipitation is represented using the mass flux scheme of Grell (1993), while radiative transfer is computed using the radiation package of the NCAR Community Climate Model, version CCM3 (Kiehl et al. 1996). This scheme describes the effect of different GHG, cloud water, cloud ice and atmospheric aerosols (see later). Cloud radiation is calculated in terms of cloud fractional cover and cloud water content, and a fraction of cloud ice is diagnosed by the scheme as a function of temperature.

## 2.3 Simulation design and observed data

The reference simulation covers the 30-year period of 1961–1990. The experiment design is as follows. The HadAMH simulation used to drive the RegCM utilizes observed SST and sea-ice distribution from the Hadley Centre HadISST dataset (Rayner et al. 2003). Time-varying (at 10-year intervals) and spatially uniform atmospheric concentrations of GHG ( $CO_2$ ,  $CH_4$ ,  $N_2O$  and  $CFCs$ ) for the period 1961–1990 are used, as provided by the Hadley Centre (Johns et al. 2001). HadAMH also includes a sulfur cycle module which, from the time varying emission of  $DMS$  and  $SO_2$  (Johns et al. 2001), computes three dimensional, time evolving fields of sulfate aerosol concentration. The module includes sources, transport, chemical transformations and removal as well as the direct and indirect (type I) radiative effects of sulfate aerosols (Johns et al. 2001).

In order to be run, the RegCM requires initial and time evolving lateral boundary conditions for wind components, temperature, water vapor mixing ratio and surface pressure. These are interpolated into the model lateral buffer zone (12 grid points) from the HadAMH fields at 6-hourly intervals. The lateral boundary condition procedure employs a standard relaxation method with an exponentially varying weighting function (see Giorgi et al. 1993b). It is important to point out that, for most PRUDENCE regional model simulations (including ours), the HadAMH forcing data were not provided on the original grid but on a coarser  $2.5^\circ$  latitude by  $3.75^\circ$  longitude grid. As a result, the effective topography and landuse of the forcing data is that of the coarser grid.

Also needed by the RegCM are the SST, sea ice and GHG concentrations throughout the simulation and the initial soil water and soil temperature. These are interpolated from the corresponding HadAMH fields. Finally, sulfate aerosols are included in the simulations. Although the RegCM has an option to incorporate an anthropogenic sulfur scheme (Giorgi et al. 2002, 2003), for consistency with the HadAMH simulation, three-dimensional sulfate concentrations in the RegCM are directly interpolated from HadAMH at six hourly intervals. From the three dimensional sulfate concentrations, the RegCM radiative transfer scheme computes the direct sulfate radiative forcing as described in Giorgi et al. (2002). Note that the calculation of the direct aerosol forcing in the model includes the effect of relative humidity on the particle size. A simplified treatment of the type I indirect aerosol forcing is also included by allowing the effective cloud droplet radius to decrease over the continents in response to greater aerosol loadings as described in Kiehl et al. (1996).

The RegCM domain and topography are shown in Fig. 1. The domain covers continental Europe and the Mediterranean Basin at a 50 km grid interval. Compared to other PRUDENCE models (e.g., Christensen and Christensen 2003), our domain is slightly shifted to the south because we cover the entire Mediterranean area and surrounding regions. Figure 1 also shows 13 subregions selected for more detailed analysis. Note that these subregions are smaller than those used in previous RegCM studies (e.g. Giorgi and Marinucci 1996b), implying a more stringent test of regional performance. The model is run at its standard vertical configuration of 14 sigma levels, model top at 80 hPa and five levels below about 1500 m. The surface vegetation and landuse types are obtained from a global dataset derived by the United States Geological Survey from satellite information (e.g., Loveland et al. 1991).

We use two observation datasets for the validation of surface air temperature and precipitation. The first was produced by the Climatic Research Unit (CRU) of the University of East Anglia (New et al. 1999, 2000). This includes monthly data of temperature and precipitation over land at a regular  $0.5$  degree resolution grid for the period 1901–2001, out of which we extracted data for

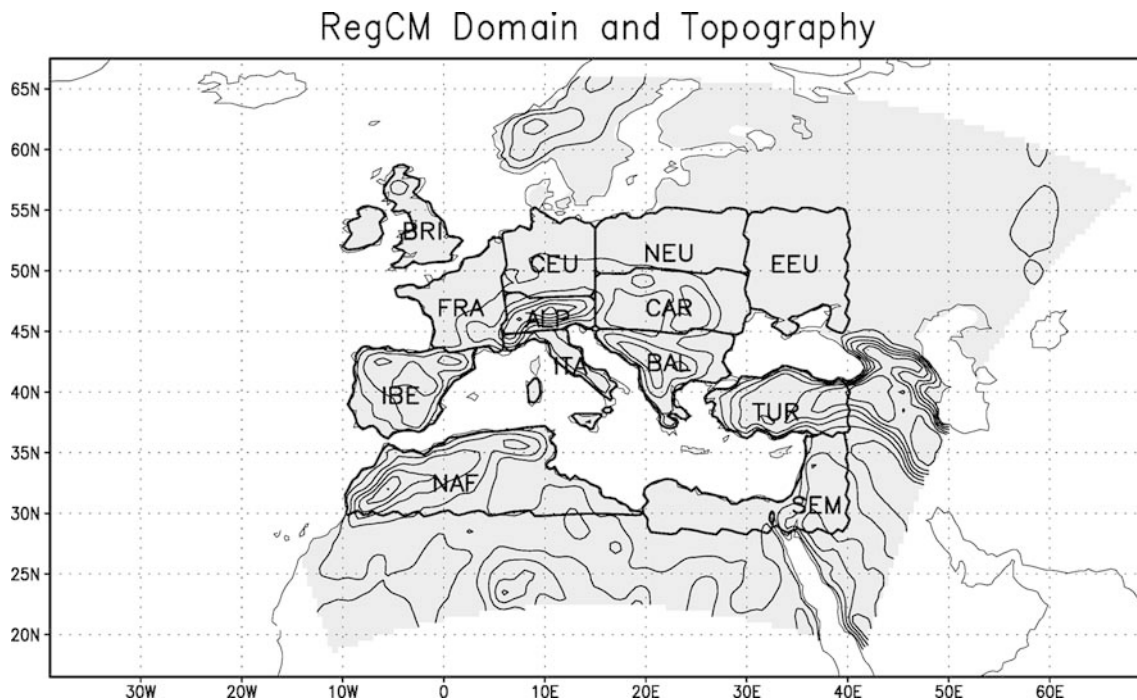


**Fig. 1** Model domain and topography. Units are m and the contour interval is 300 m. Also shown are 13 subregions used for more detailed analysis. *IBE*, Iberian Peninsula; *ITA*, Italian Peninsula; *BAL*, Balkan Peninsula; *TUR*, Turkey; *NAF*, Northwest

Africa; *SEM*, Southeastern Mediterranean; *ALP*, Alps; *FRA*, France; *BRI*, British Isles; *CEU*, Central Europe; *CAR*, Carpathian region; *NEU*, Northeastern Europe; *EEU*, Eastern Europe

1961–1990 for comparison with the model simulation. New et al. (1999, 2000) provide estimates of the uncertainty associated with the CRU climatology using both an internal cross-validation procedure and a comparison with other available observed climatologies. They conclude that uncertainties in observed climatic averages for multi-decadal periods are of the order of 0.5–1.3 °C for temperature and 10–25% for precipitation, and are largest over regions characterized by poor station coverage and high spatial variability, such as for example in many mountainous areas.

The second dataset is that of Willmott and Matsuura (2001), hereafter referred to as WM. This consists of monthly half degree resolution land observations of surface air temperature and precipitation for the period 1950–1999, out of which we extracted data for 1961–1990. In the calculation of the precipitation average, however, we added to the original data the gauge correction of Legates and Willmott (1990). This is done because Adam and Lettenmaier (2003) emphasized that observed precipitation data are characterized by a systematic underestimation, most noticeably because of wind-induced gauge undercatch of solid precipitation. Precipitation can also be underestimated because of wind-induced undercatch of liquid precipitation and wetting losses, although these effects are less important. The estimated bias due to the undercatch varies from less than 10% in the warm season to more than 20% in the Northern Hemisphere winter months at mid to high latitudes.

Both the CRU and WM datasets do not account for gauge undercatch and when regionally and decadal

averaged, they yield similar values. The addition of the gauge correction to one of the datasets thus allows an estimate of the uncertainty associated with the gauge undercatch. Because we add the gauge correction of Legates and Willmott (1990) to the average data of WM we refer to the corrected dataset as WM/LW. Note that the gauge correction is climatological and varies from month to month throughout the year. Also, in the comparison of observations and simulations, all data are interpolated onto the RegCM grid.

Finally, for the validation of atmospheric variables we use fields from the NCEP (National Center for Environmental Prediction) reanalysis, which covers the entire period 1961–1990 at a horizontal grid interval of 2.5 degrees (Kalnay et al. 1996).

## 2.4 Measures of analysis

A series of measures of analysis are employed here for model validation. As a measure of the model systematic error we use the model bias, which is defined as the difference between the 30-year average simulated and observed fields. Climatic trends are measured by the linear trend value obtained from a least square fit line to the full 30 years of data. The basic measure of interannual variability is the temporal standard deviation, *STDV*, defined (e.g. for temperature) by

$$STDV = \sqrt{\frac{\sum_i (T_i - \bar{T})^2}{N - 1}} \quad (1)$$

where  $N = 30$  (years) and  $\bar{T}$  is the 30-year average temperature. For precipitation the standard deviation is normalized by the 30-year average, therefore it is effectively a coefficient of variation (CV). This is done because the precipitation standard deviation is typically affected by the mean, so that the coefficient of variation is a more independent measure of interannual variability.

In the comparison of observations and simulations, all data are interpolated onto the RegCM grid. All the measures defined in this section are calculated at individual grid points and then, when needed, are averaged over the subregions of Fig. 1. Only land points are considered in the analysis, and the seasons are defined as December–January–February (DJF), March–April–May (MAM), June–July–August (JJA) and September–October–November (SON).

### 3 Results

#### 3.1 Seasonal means and biases

We begin our analysis with a comparison of the average DJF and JJA 500 hPa heights and winds between the RegCM and the NCEP reanalysis for 1961–1990 (Fig. 2). The corresponding HadAMH fields were very close to those of the RegCM, both for geopotential height and wind circulation, and thus they are not shown here. As noted in previous nested modeling work, this is because the large-scale mid-tropospheric circulations in a regional model are primarily controlled by the forcing boundary conditions.

Overall, the models (both RegCM and HadAMH) underestimate the 500 hPa geopotential height compared to the NCEP reanalysis throughout the domain in both seasons, an indication of generally colder tropospheric temperatures. However, the observed height gradients and associated wind circulations are reproduced reasonably well in the simulations, both in their spatial patterns and seasonal evolution. In the winter, a ridge dominates over the western European regions and a trough over the Eurasian continental areas. The model locates the ridge about  $10^\circ$  to the east of the observed, but overall the observed wave pattern is reproduced. In the summer, the sub-tropical high moves northward over northern Africa and a trough deepens over the Eastern Mediterranean. In the simulation, the northern African high is displaced a little south of the observed and the Eastern Mediterranean trough is somewhat deeper than observed, but also in JJA the basic observed large-scale wave structure is captured. The differences between observed and simulated average circulations appear to be most pronounced in the northern regions of the domain, which could affect the simulated climate over Scandinavia and the Baltic region. A general agreement between simulation and observations and between the RegCM and HadAMH experiments was also found in MAM and SON (not shown).

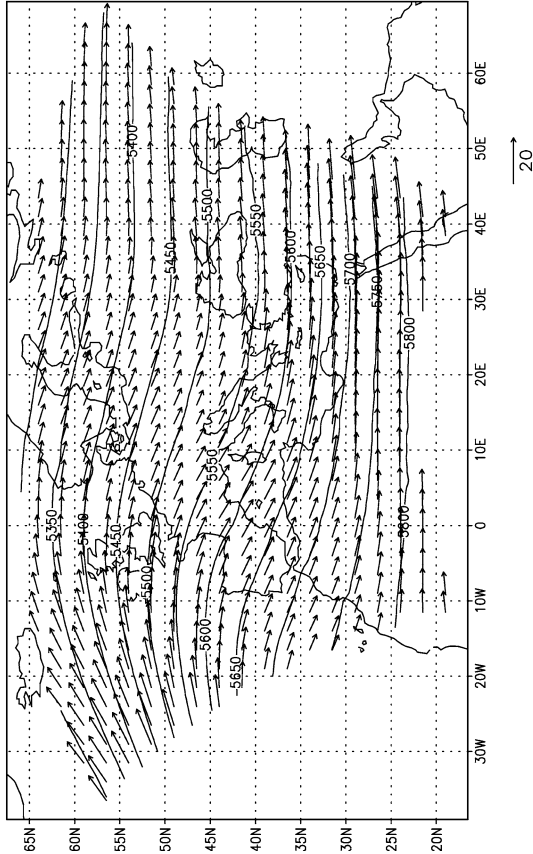
Figure 3 compares the 30-year average seasonal surface air temperature in the CRU observations and the RegCM simulation. Data are shown only for the interior of the domain in order to more clearly illustrate the fine scale topographically-induced detail. The broad spatial patterns of HadAMH surface air temperatures are not shown since they were similar to those found in the RegCM simulation. Overall, the regional model reproduces well the observed regional patterns of surface air temperature and their seasonal evolution. The topographically induced regional detail, which is of the same scale in the CRU and RegCM data, is also captured. In general, the RegCM appears characterized by a predominant cold bias of a few degrees in MAM and SON, a predominant warm bias in JJA and more mixed biases in DJF.

Quantitative estimates of the model temperature biases can be obtained from Fig. 4, which presents CRU and WM observations and RegCM and HadAMH simulated temperatures averaged over the different subregions of Fig. 1. In this regard, the comparison with the HadAMH fields should be considered mostly as illustrative because, although these fields were interpolated onto the RegCM grid, the land areas in the RegCM and HadAMH are different and this can affect the subregional averages in coastal regions. Also, it is evident from Fig. 4 that the CRU and WM observed temperatures are very close to each other. Figure 4 indicates that the regional biases in the RegCM simulation are smaller than  $2^\circ\text{C}$  in the vast majority of cases and in fact in many cases they are smaller than  $1^\circ\text{C}$  (9 or 10 out of 14 subregions in DJF, JJA and SON, and 4 out of 14 subregions in MAM), with MAM being the season of largest biases.

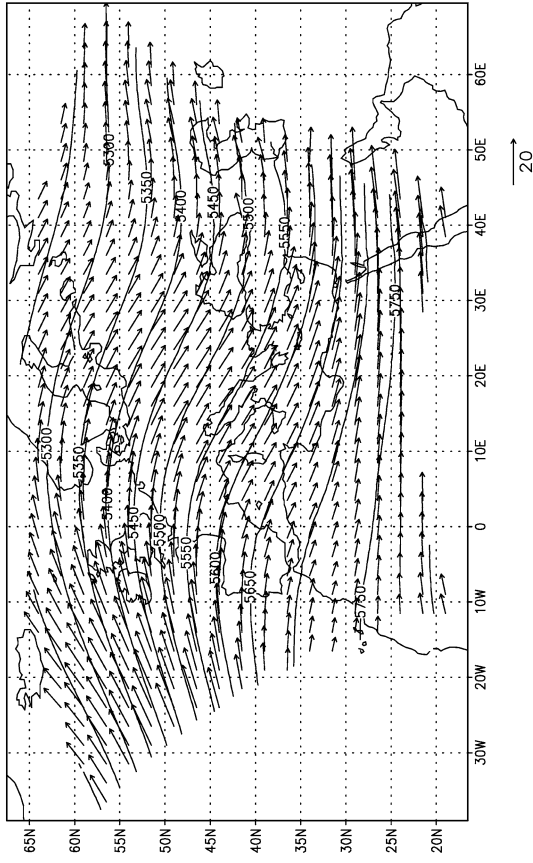
As a general consideration, in the evaluation of the temperatures in Fig. 4 it should be recalled that at least in mountainous regions (e.g., ALP and TUR) the observed data may be affected by a warm bias due to the prevalence of low elevation and valley stations compared to high elevation ones (New et al. 1999, 2000). In addition, the models do not include urban effects, which may also affect the observations in highly urbanized regions.

The subregional biases in the HadAMH simulation are of similar magnitude as in the RegCM simulation, but they have a different seasonal distribution. In fact, in contrast to the RegCM, the HadAMH simulation is characterized by surface temperatures predominantly warmer than observed, especially in DJF. This is due to a feature evident in Fig. 4, i.e., that the near-surface air temperature over land appears systematically lower in the RegCM than in HadAMH, by order of several tenths of a degree to a few degrees in different subregions of the domain. To gain an understanding of this result, Fig. 5a,b shows the vertical profile of the difference between RegCM and HadAMH temperature and water vapor mixing ratio averaged over all land areas encompassed by the 13 land regions of Fig. 1. Fig. 5a,b shows that the RegCM is colder and drier than the

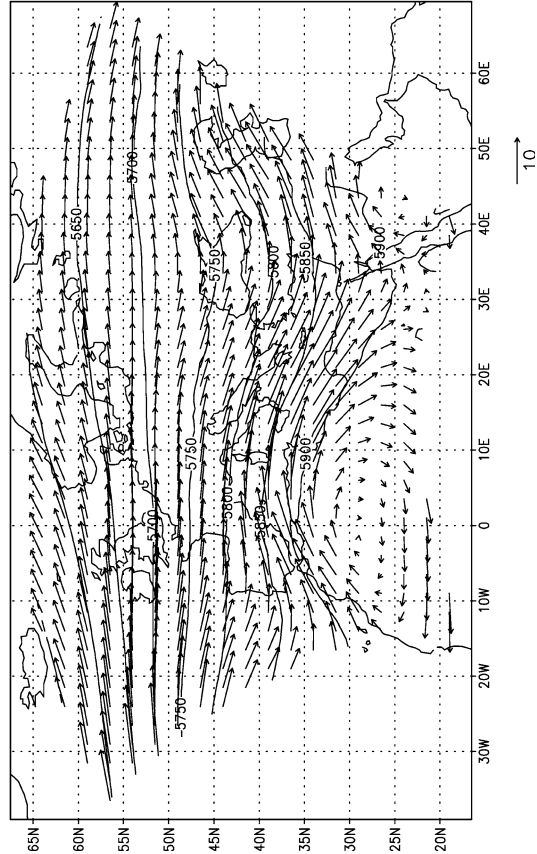
(a) 500HPa, AVE, NCEP, DJF, 1961\_1990



(b) 500HPa, AVE, RegCM, DJF, 1961\_1990



(c) 500HPa, AVE, NCEP, JJA, 1961\_1990



(d) 500HPa, AVE, RegCM, JJA, 1961\_1990

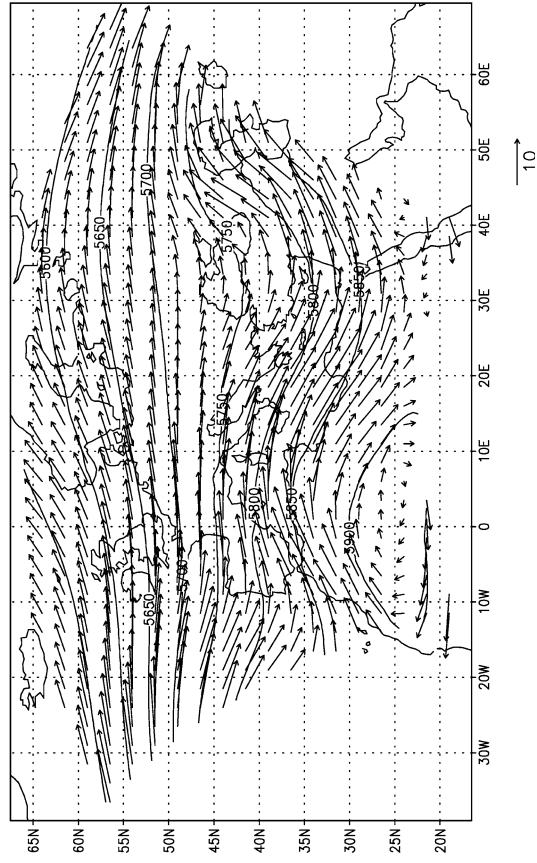




**Fig. 2** Average geopotential height (m) and wind (m/s) at 500 hPa. **a** DJF, NCEP reanalysis; **b** DJF, RegCM simulation; **c** JJA, NCEP reanalysis; **d** JJA, RegCM simulation

HadAMH in the boundary layer and lower troposphere and it is warmer and moister in the mid to high troposphere.

These results indicate that the RegCM has a more efficient vertical transport of energy and water vapor from the boundary layer to the free troposphere. One reason for this behavior is the use of different planetary boundary layer schemes in the models. The RegCM adopts a non-local boundary layer representation in which the vertical eddy diffusion coefficient follows a prescribed profile between the surface and the boundary layer top, which is calculated from the bulk stability of the lower troposphere (Holtslag et al. 1990). In other words, in this non-local scheme the vertical diffusion depends on the bulk stability of the boundary layer. Conversely, HadAMH adopts a local formulation in which the vertical diffusion coefficient depends on the local thermal stability (Pope et al. 2000). Giorgi et al. (1993a) showed that non-local schemes tend to enhance vertical heat and moisture transport compared to local schemes, thereby leading to a relative cooling and drying of the surface.

A second reason for the difference profiles of Fig. 5 may be attributed to the use of different convection schemes. The net effect of convection is to redistribute vertically, and in particular transport upward, energy and moisture. As seen in Sect. 2, both HadAMH and the RegCM use mass flux cumulus convection schemes. However, the schemes adopt different closures and parameter assumptions, and as a result their efficiency in redistributing heat and moisture may be different. This effect would be especially important in the warm season, when cumulus convection is more active.

A third contribution to the lower near-surface temperatures and water vapor amounts in the RegCM could also derive from the land surface process schemes, which are different in the models. The RegCM uses the BATS scheme, while HadAMH adopts the scheme of Cox et al. (1999). Several components of the land surface schemes may contribute to the differences in surface air temperature between the models, for example the treatment of the drag coefficient, the transpiration process, or the simulation of the cycle of snow formation and melting, and it is difficult to identify which of them might be important. Regardless of the specific cause of the difference in lower level temperatures between the RegCM and HadAMH this appears to be a systematic effect.

Figures 6a–h compares the average CRU and RegCM precipitation in the interior model domain for the four seasons. In DJF (Fig. 6a) the Mediterranean region experiences its wet season characterized by a maximum in the frequency of storms crossing the region. The North Atlantic storm track also induces heavy precipitation

over the western and northern European regions. With the onset of the warm season (Fig. 6e), the storm track progressively migrates to the north, inducing wet conditions over central Europe and dry conditions over the Mediterranean basin. Intermediate conditions are found in MAM and SON (Fig 6c and g, respectively). As shown by Fig. 6, the RegCM experiment captures the broad spatial pattern of precipitation and its seasonal evolution. This is the case also for the HadAMH simulation (not shown for brevity), although HadAMH obviously exhibits less high-resolution detail. HadAMH is thus successful in capturing the seasonal evolution of the primary storm tracks affecting the European region and transmits this information to the RegCM through the lateral boundary forcing.

Observed precipitation shows a number of topographically induced fine scale regional features, such as maxima over the Alpine, Balkan and Carpathian regions, and the western coastal ranges of the Iberian Peninsula, the British Isles and the Scandinavian Peninsula. These features are evident in all seasons, although with varying magnitudes. The RegCM successfully reproduces these regional maxima in all seasons, although their simulated intensity may differ from observations. In particular a tendency is noted in the RegCM to produce larger precipitation amounts than in the CRU observations, generally throughout the simulation and in particular over some of the topographical chains in the warm season.

A quantitative evaluation of the precipitation simulation over different subregions is given in Fig. 7, which presents the regional precipitation averages calculated from the two observed and modeled datasets. As discussed in Sect. 2, the WM/LW dataset includes a correction to account for the gauge undercatch of precipitation and it is interesting to first compare the regional precipitation amounts in the two observed datasets. The WM/LW precipitation is consistently higher than the CRU precipitation in all regions and seasons, with the exception of a few regions in JJA. The gauge correction is maximum in DJF and over eastern European and mountainous regions, where the DJF precipitation is higher in the WM/LW data than in the CRU data by up to 25–35%. Overall, when averaging over all regions, the DJF precipitation is higher in the WM/LW data than in the CRU data by about 25%. Also in MAM and SON the gauge correction is substantial over a number of regions and, when averaged over all regions, it amounts to about 12% in MAM and 15% in SON.

It is also interesting to compare the RegCM and HadAMH precipitation amounts. A systematic difference between the two models is noted by which the RegCM tends to produce greater precipitation than HadAMH. This may be due to different causes. First, Giorgi and Marinucci (1996a) showed that the simulation of precipitation may be sensitive to the model resolution regardless of the topographic forcing. In particular, in their experiments precipitation tended to

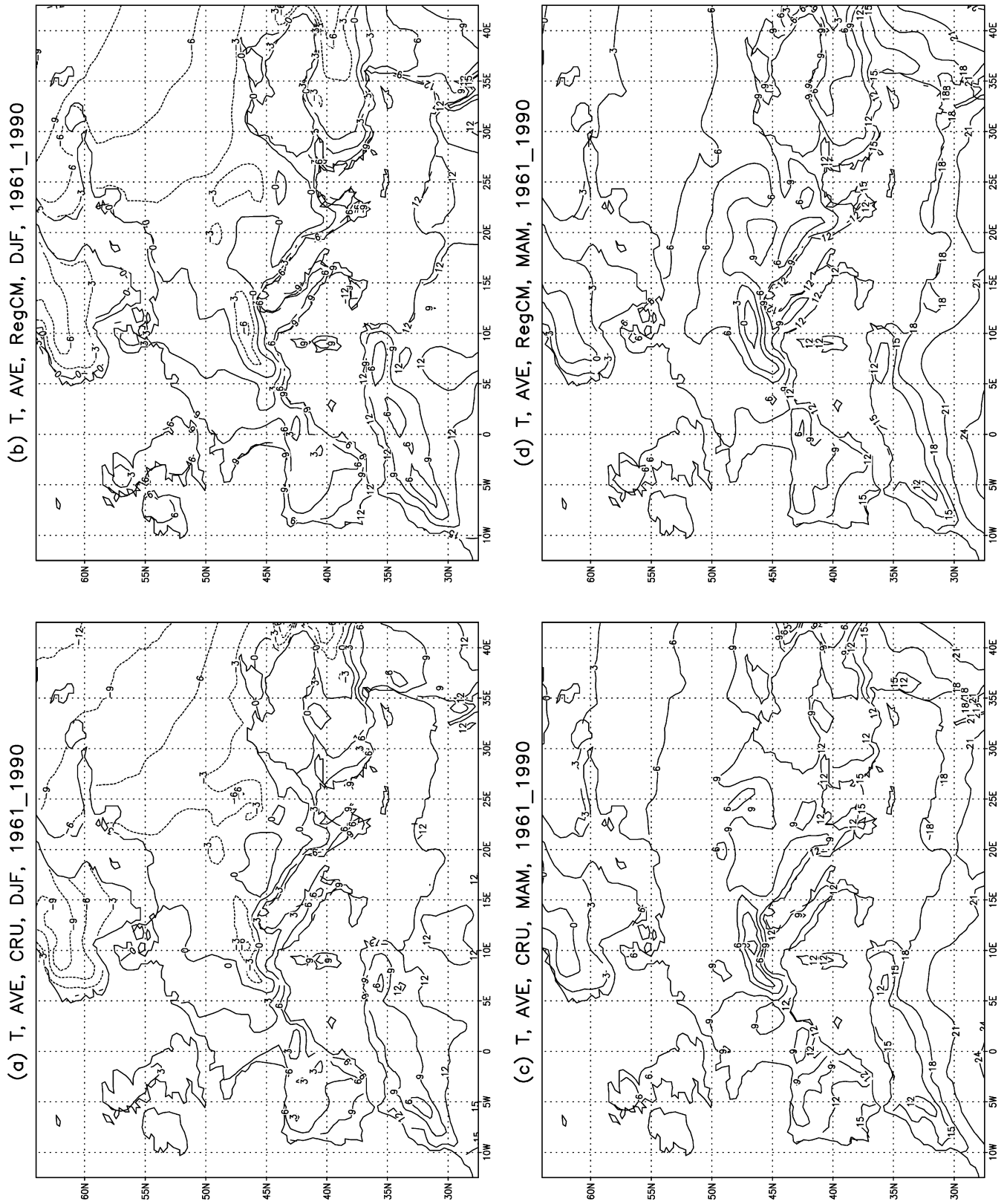


**Fig. 3** Observed (CRU) and simulated (RegCM) average surface air temperature for the period 1961-1990 in the interior model domain. **a** DJF, CRU; **b** DJF, RegCM; **c** MAM, CRU; **d** MAM,

RegCM; **e** JJA, CRU; **f** JJA, RegCM; **g** SON, CRU; **h** SON, RegCM. Units are degrees C and the contour interval is 3 °C



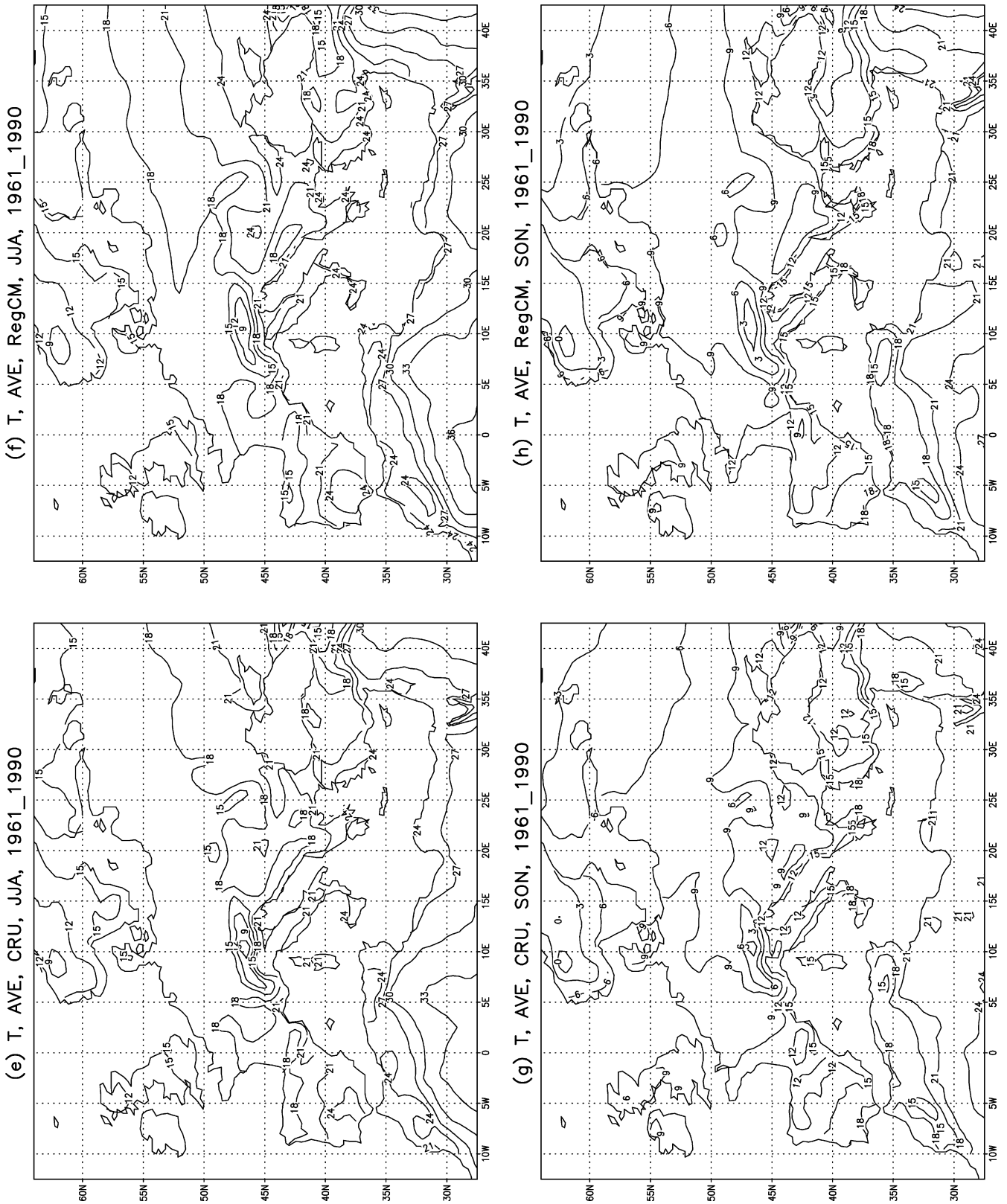
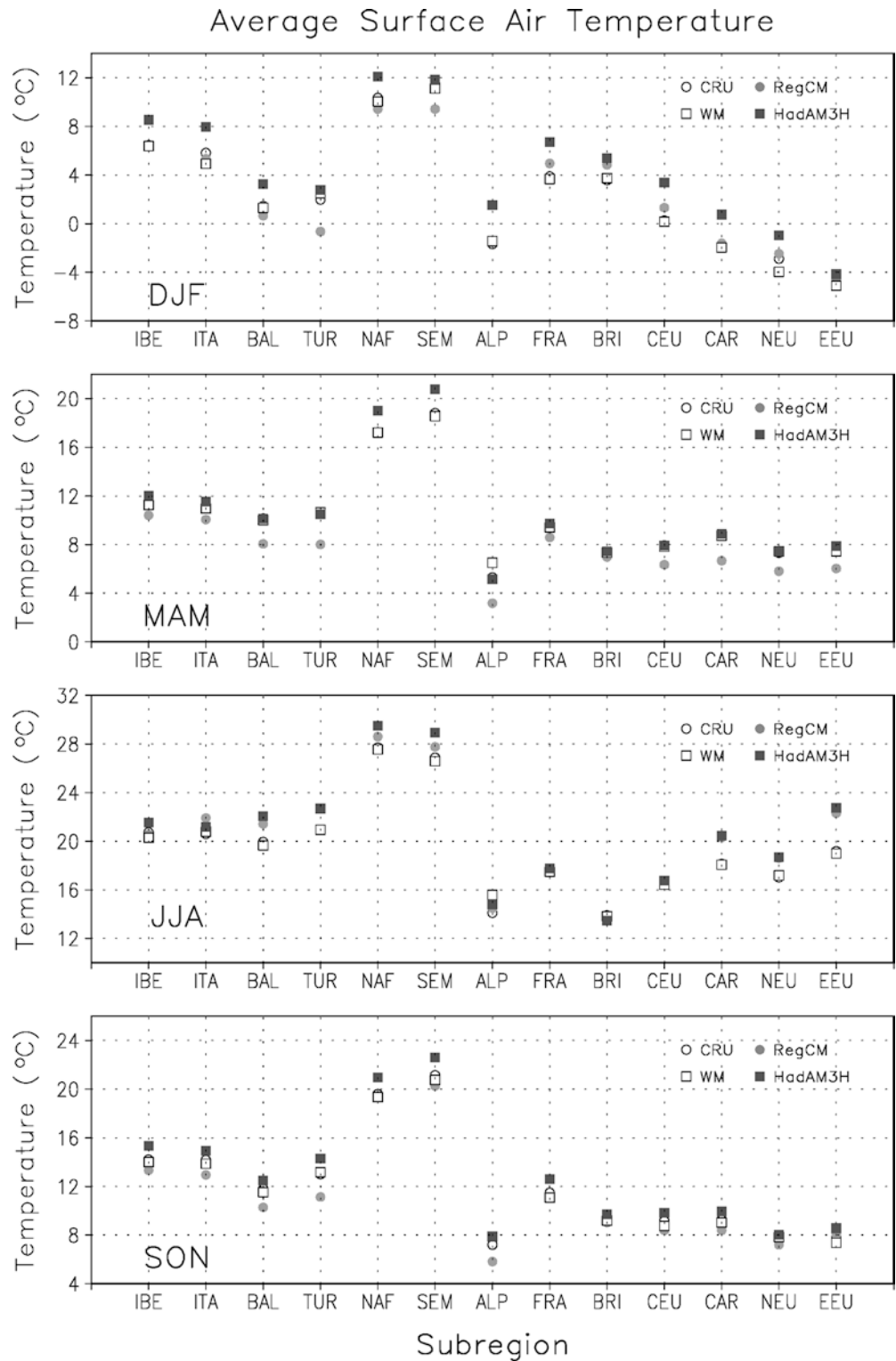


Fig. 3 (Contd.)

increase at finer resolutions. Greater topographic forcing at higher resolution would then further strengthen this effect. The greater vertical transport of water vapor

in the RegCM (Fig. 5b) may also contribute to greater precipitation amounts by enhancing uplift and subsequent condensation of water vapor. Finally, the

**Fig. 4** Observed (CRU and WM) and simulated (RegCM and HadAMH) seasonal surface air temperature averaged over the 13 subregions of Fig. 1. Only land data are included in the regional average. Units are degrees C. Seasons are DJF, MAM, JJA and SON in order from the *top* to the *bottom* panel



different convection schemes in the models may be characterized by different precipitation efficiencies.

Overall, Fig. 7 indicates that the RegCM simulation tends to overestimate precipitation when compared to the CRU data, with MAM being the season with the most pronounced overestimate. The RegCM precipitation is more in line with the gauge corrected WM/LW

observations except in MAM, when a precipitation overestimate is still found. Conversely, the HadAMH simulated precipitation is more in line with the CRU observations, with a tendency to underestimate precipitation in JJA, especially over the Alpine region. The seasonal precipitation bias in the RegCM compared to the CRU dataset is less than 25% in the majority of

## RegCM–HadAM3H, Land Only

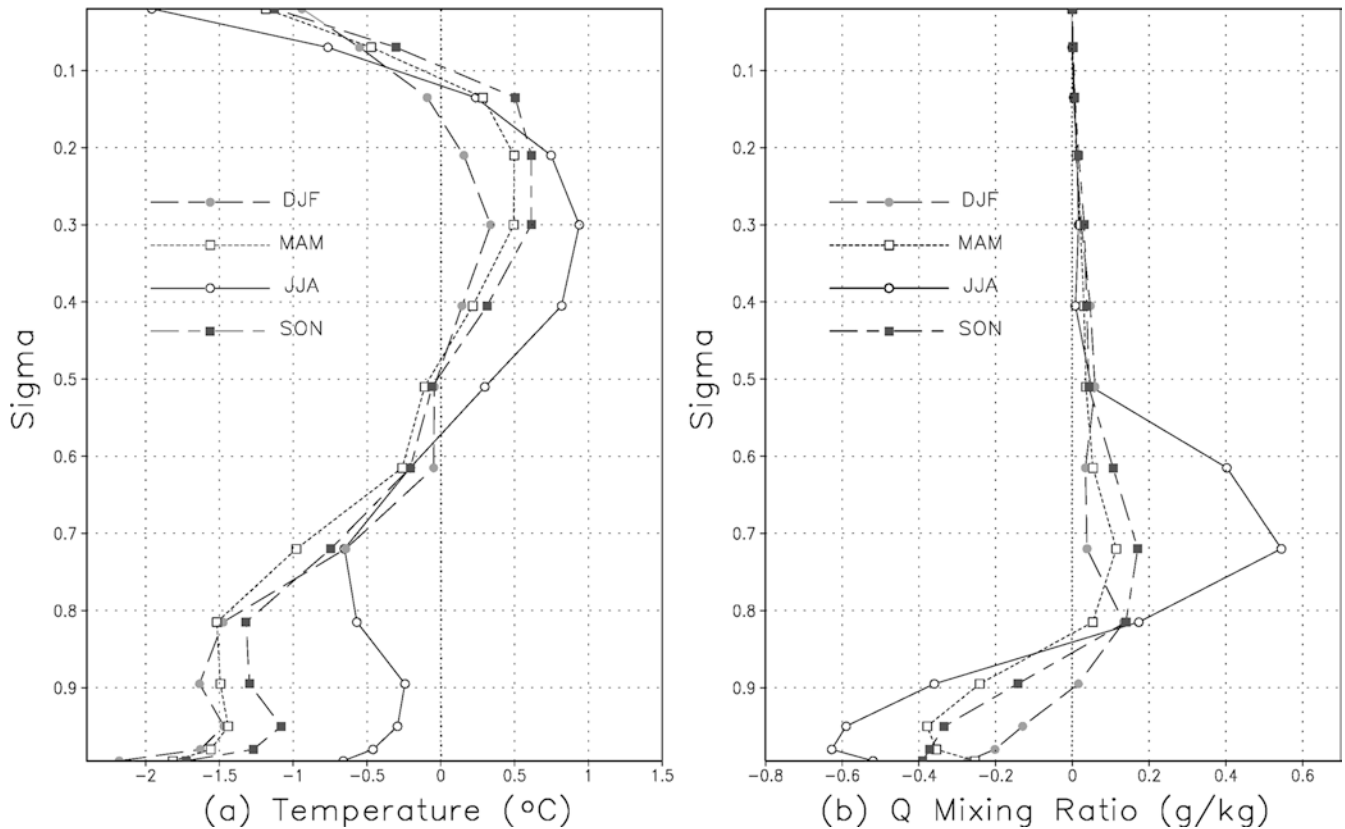


**Fig. 5** Vertical profile of the difference between RegCM and HadAMH average **a** temperature and **b** water vapor mixing ratio ( $Q$ ). The average is taken over all land points included in the 13

subregions of Fig. 1. Units are degrees C for temperature and g/kg for the mixing ratio

cases, with a number of cases of larger bias in MAM. The biases are smaller compared to the WM/LW dataset, with magnitudes mostly less than 10–20%. Similarly, the regional biases in HadAMH are generally less than 10–20%. Considering the uncertainties indicated by New et al. (1999, 2000) and those implied by the use of a gauge undercatch correction, in both models the biases are mostly of the same order of magnitude as the observation uncertainties (10–30%).

In summary, overall the average climatology of this simulation, both for HadAMH and RegCM, is of relatively good quality when compared with previous experiments (e.g., Marinucci and Giorgi 1992; Giorgi and Marinucci 1996b; Jones et al. 1995), especially when we consider that the size of the subregions analyzed is smaller than in previous studies, which implies a more stringent test of the model performance.

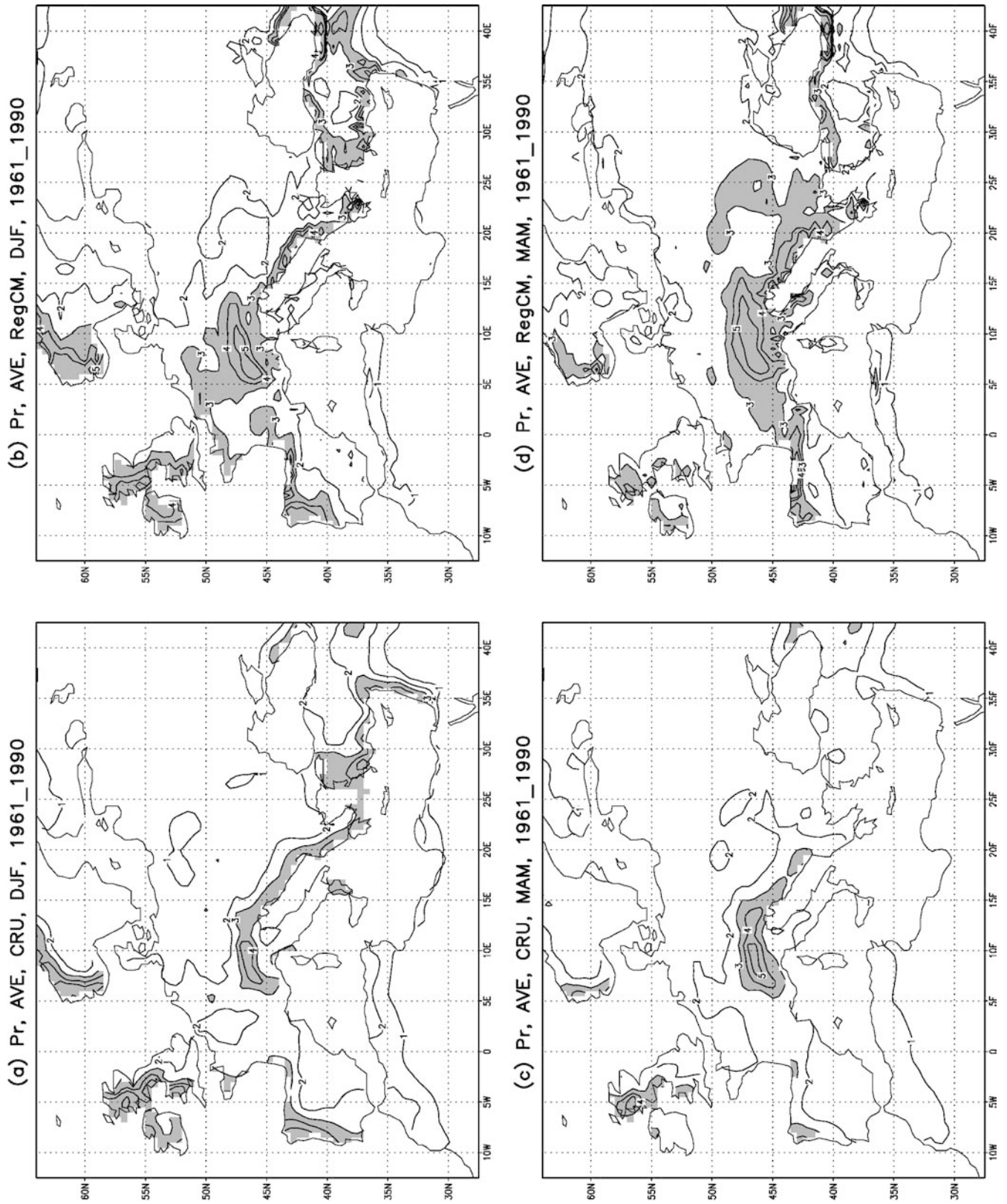
### 3.2 Interannual variability

Figure 8 shows the interannual standard deviation of surface air temperature in the CRU and WM observations and in the RegCM and HadAMH simulations averaged over the 13 subregions of Fig. 1. The regional

values were obtained by first calculating the standard deviation at each grid point and then averaging it over all the land grid points of the regions.

The observed temperature standard deviation, and thus the interannual variability, is maximum in the winter over the northern and northeastern European regions (EEU, CEU, CAR, NEU). In DJF the temperature standard deviation varies in the range of 0.8 °C over the western European coastal regions to about 2.5 °C in northeastern Europe. In the other seasons the observed standard deviation is more homogenous throughout Europe and varies in the narrower range of 0.6 to 1.7 °C in MAM and 0.5 to 1.2 °C in JJA and SON. Similarly to DJF, also in the other seasons the interannual variability is somewhat greater over the central and northeastern European regions, whose climate is less affected by the less variable ocean temperatures.

A general agreement is found between the temperature standard deviations in the CRU and WM observed datasets, although the latter shows somewhat greater variability over the Mediterranean regions. Note that, even when using the same set of observing stations, differences between observed datasets can be attributed to the smoothing and interpolation procedure used to generate gridded data from station values.



**Fig. 6** Observed (CRU) and simulated (RegCM) average precipitation for the period 1961-1990 in the interior model domain. **a** DJF, CRU; **b** DJF, RegCM; **c** MAM, CRU; **d** MAM, RegCM;

**e** JJA, CRU; **f** JJA, RegCM; **g** SON, CRU; **h** SON, RegCM. Units are mm/day and the contour interval is 1 mm/day. *Shading* indicates values greater than 3 mm/day

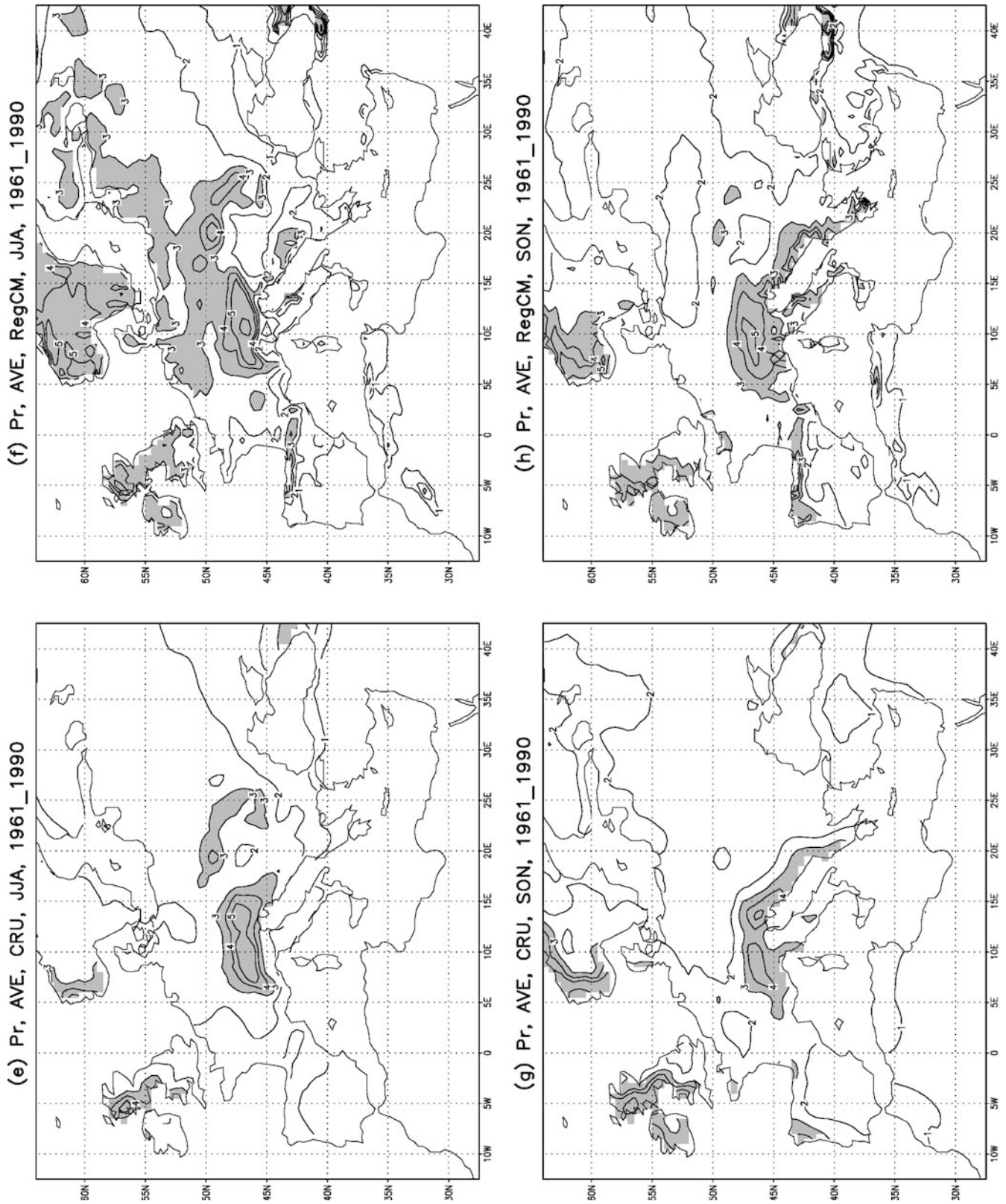
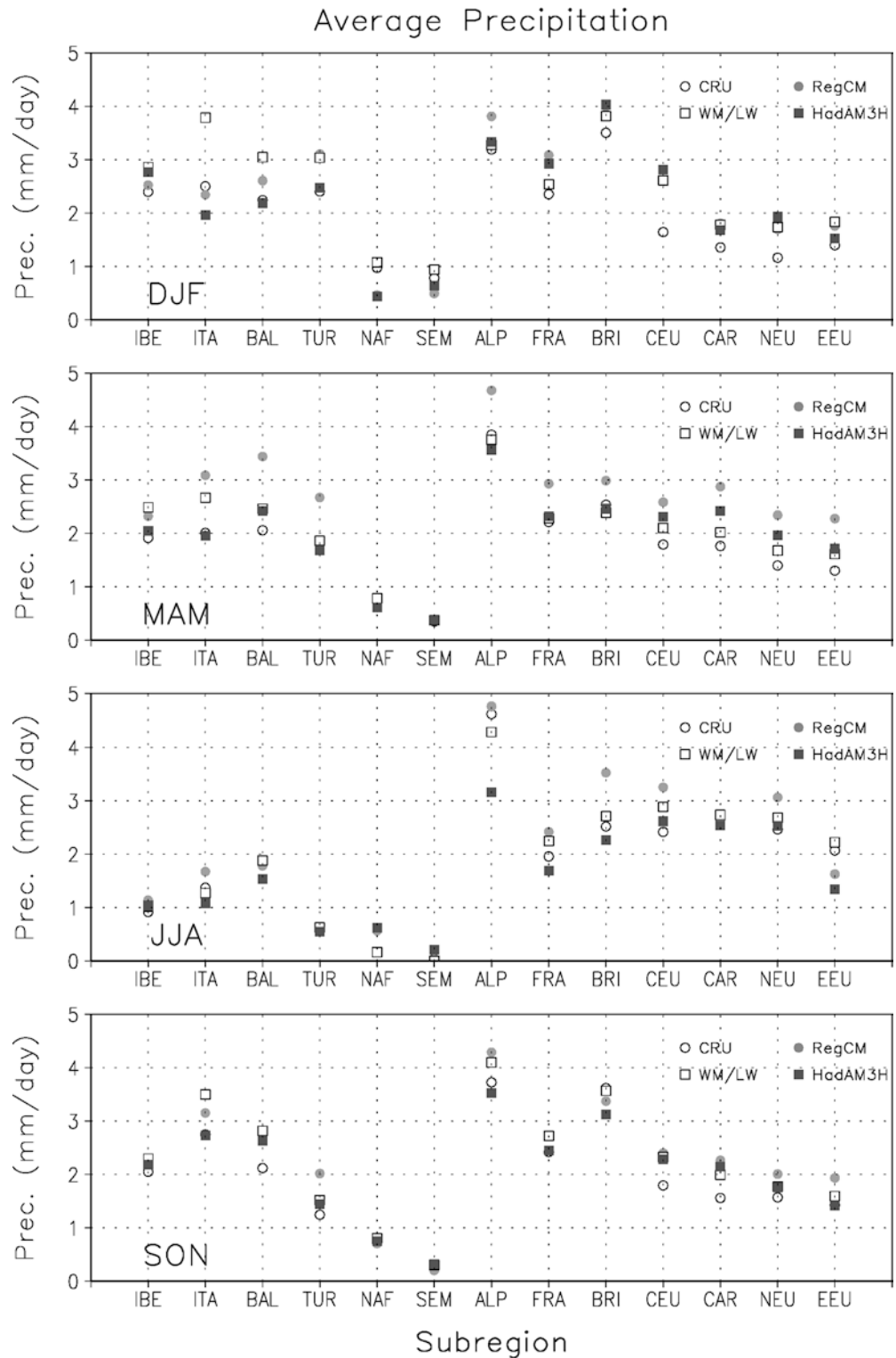


Fig. 6 (Contd.)

Compared to the observations, both the RegCM and HadAMH tend to underestimate the DJF surface temperature interannual variability over a number of re-

gions of western, central and eastern Europe. Over the EEU and NEU regions, the standard deviations are significantly higher in HadAMH than in the RegCM.

**Fig. 7** Observed (CRU and WM/LW) and simulated (RegCM and HadAMH) seasonal precipitation averaged over the 13 subregions of Fig. 1. Only land data are included in the regional average. Units are mm/day. Seasons are DJF, MAM, JJA and SON in order from the *top* to the *bottom* panel

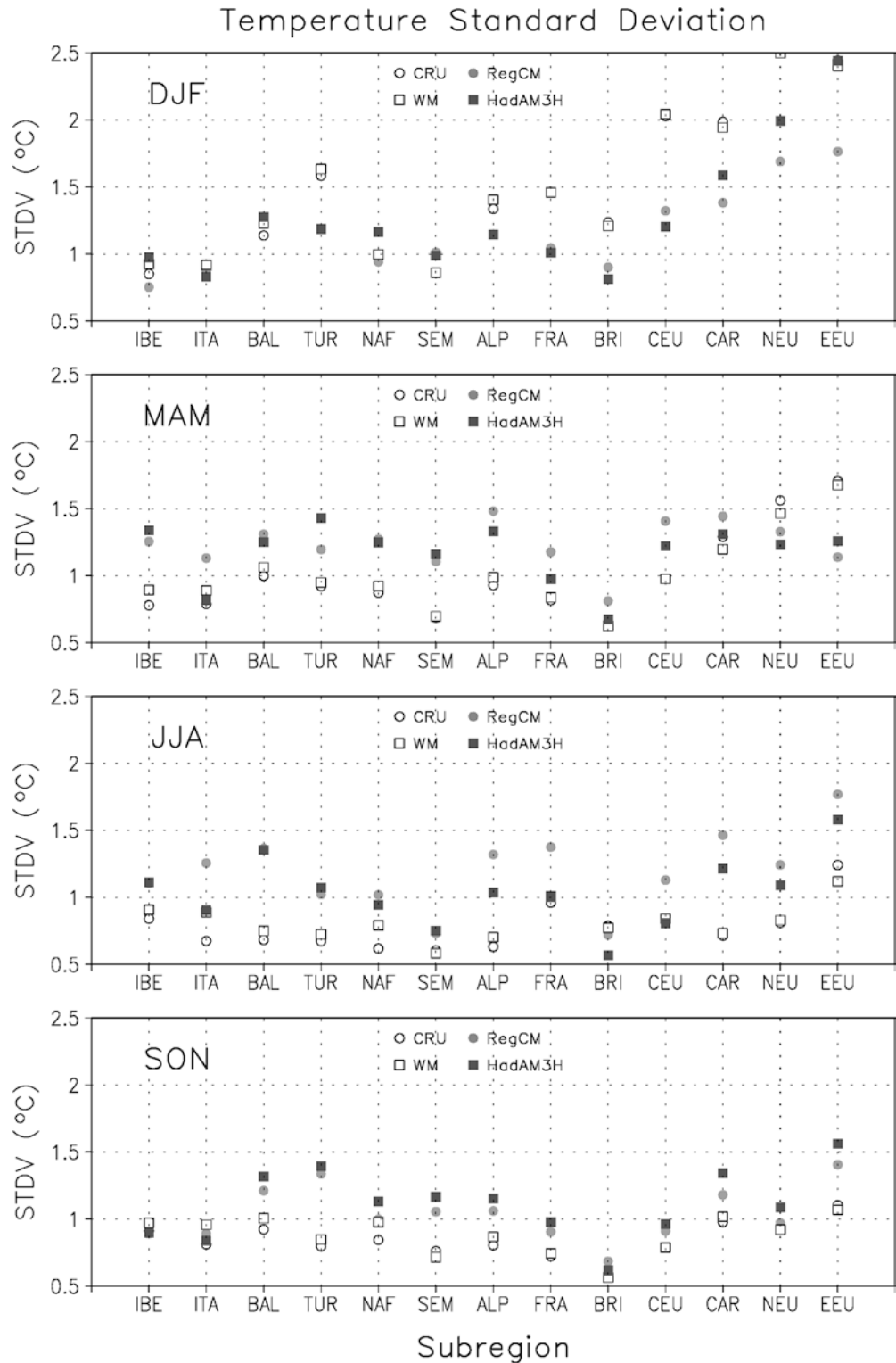


Over these regions, in the winter the interannual variability is modulated by the snow albedo feedback mechanism (e.g., Giorgi 2002a,b), so that this difference between HadAMH and RegCM may be related to less variable amounts of snow in the regional model.

In the other seasons the models appear to mostly overestimate the observed temperature variability,

especially in MAM and JJA. In the mid-seasons the standard deviations in the RegCM and HadAMH are generally close to each other, a sign that the nested model is inheriting a good portion of its temperature interannual variability from HadAMH. In JJA, however, the RegCM is characterized by larger temperature interannual variability than HadAMH over a number of

**Fig. 8** Observed (CRU and WM) and simulated (RegCM and HadAM3H) seasonal surface air temperature interannual standard deviation (STDV) averaged over the 13 subregions of Fig. 1. Only land data are included in the regional average. Units are degrees C. Seasons are DJF, MAM, JJA and SON in order from the *top* to the *bottom* panel

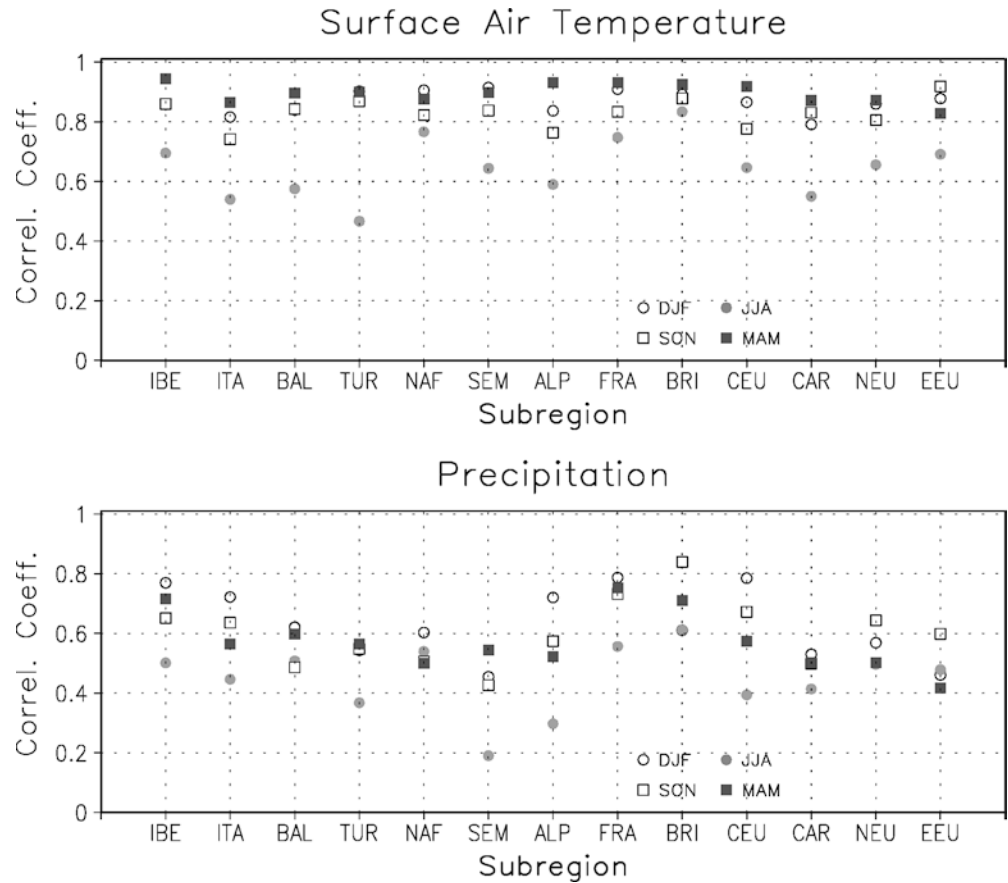


regions. Giorgi (2002c) analyzed the dependence of the surface climate interannual variability on spatial scales comprising between 50 to 300 km, therefore a range encompassing the RegCM and HadAMH horizontal resolutions. He found that the temperature and precipitation interannual variability tends to increase at finer scales, most markedly in the summer. This effect can

thus contribute to the higher standard deviation values found in the RegCM summer temperatures.

To measure the degree to which the HadAMH model drives the RegCM temperature interannual variability, we calculated the interannual correlation coefficients between the RegCM and HadAMH seasonal temperature anomalies (Fig. 9). These coefficients were first

**Fig. 9** Interannual correlation coefficients between RegCM and HadAMH seasonal temperature anomalies (*top panel*) and between RegCM and HadAMH seasonal precipitation anomalies (*bottom panel*) averaged over the 13 subregions of Fig. 1



calculated at the individual grid points and then averaged over the land grid points of the 13 subregions. A high correlation indicates that the HadAMH strongly drives the interannual RegCM variability, while a low correlation indicates that the RegCM variability is more due to internal model processes. Figure 9a shows that the correlation coefficients are high, order of 0.8 or more, in DJF, MAM and SON. This indicates that even at the RegCM grid point scale, most of the interannual variability of temperature is driven by the lateral forcing from HadAMH. In JJA, however, the correlation coefficients are lower, 0.5–0.8, especially in coastal and mountainous regions. In fact, in JJA the boundary forcing explains less than 50% of the grid point temperature interannual variability (correlation coefficient less than 0.7) over most regions. Evidently, in the summer local processes are more important than the boundary forcing in determining the RegCM interannual variability.

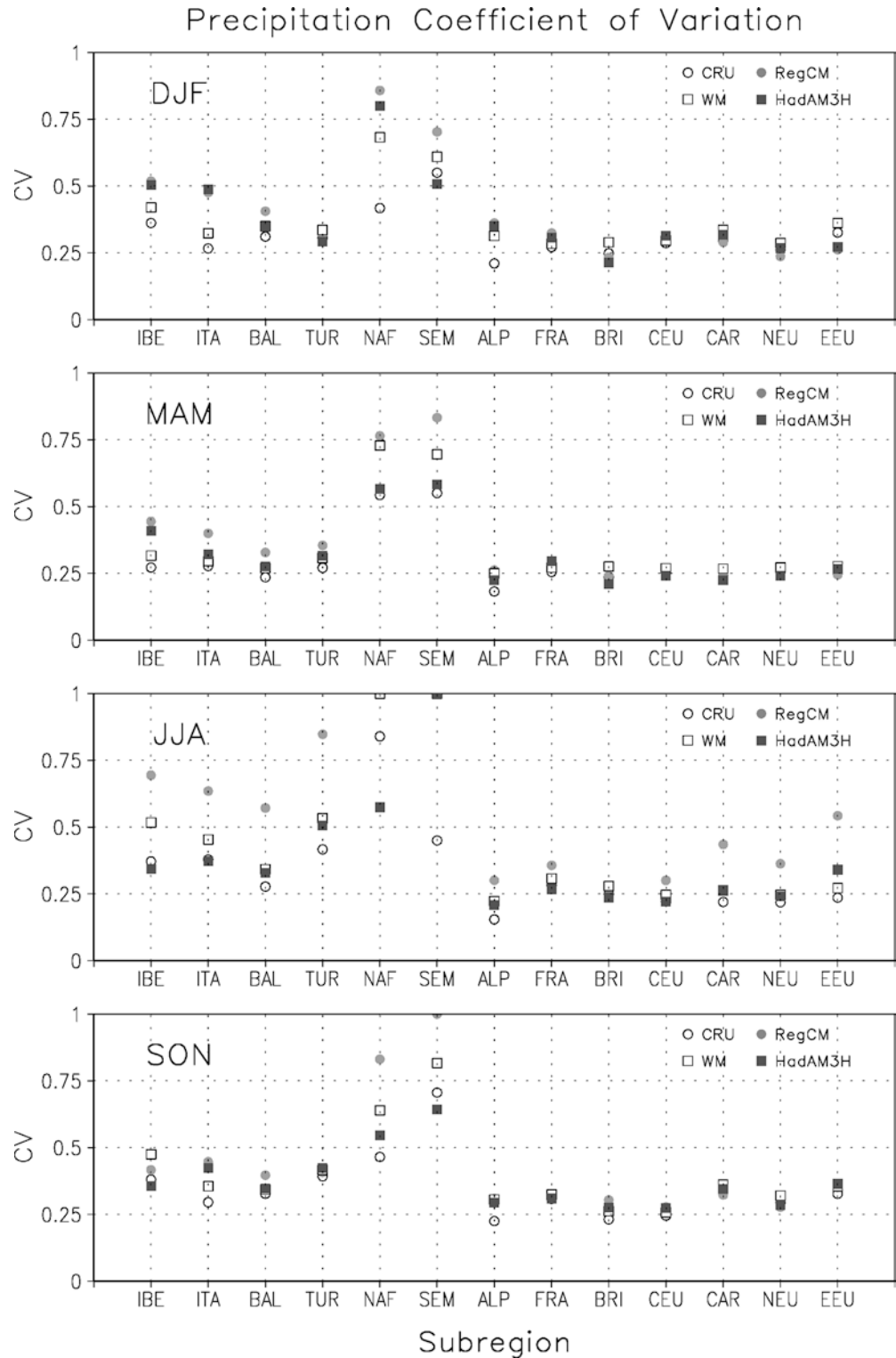
We also calculated the correlation coefficients between simulated and observed temperature anomalies, and these were generally low for both the RegCM and HadAMH. This result is not surprising since one realization cannot be expected to capture the specific anomalies of individual years but only the statistical properties of the anomalies. Similarly to seasonal and interannual prediction, ensembles of simulations are needed to evaluate a model's performance in predicting individual seasonal or yearly events.

It is also interesting to compare our results with those of Giorgi (2002a,b), who calculated the interannual standard deviation of temperature for the twentieth century over a number of broad regions, including a region covering the Mediterranean Basin and one covering central and northern Europe. The calculations were performed with the CRU dataset and with the Hadley Centre global coupled model HadCM3, whose atmospheric component is the same as that of HadAMH. Giorgi (2002a,b) found that the HadCM3 overestimated the observed temperature standard deviations over both the Mediterranean and northern European regions, and both in summer and winter. Therefore, while the HadCM3 summer results are consistent with ours, the winter results are in the opposite direction. This can likely be attributed to the ocean component of HadCM3 compared to the use of observed SSTs in HadAMH.

The precipitation coefficients of variation for the CRU and WM observations and the RegCM and HadAMH simulations averaged over the subregions of Fig. 1 are shown in Fig. 10. The observed coefficient of variation shows a relatively uniform distribution throughout Europe, with values mostly between 0.1 to 0.5. These values increase over the northern Africa regions, and this can be attributed to the effect of dividing the standard deviation by very low average precipitation amounts, especially in JJA. Overall, the interannual variability of precipitation, as measured by



**Fig. 10** Observed (CRU and WM) and simulated (RegCM and HadAMH) seasonal precipitation interannual coefficient of variation (CV) averaged over the 13 regions of Fig. 1. Only land data are included in the regional average. Units are mm/day. Seasons are DJF, MAM, JJA and SON in order from the *top* to the *bottom* panel



the coefficient of variation, does not show pronounced seasonal variations. This would not be the case when looking at the precipitation standard deviation itself, which is affected by the seasonal precipitation amounts.

When first comparing the two observed datasets, we notice that, while they generally agree over the central and eastern European regions, they show substantial

differences over the Mediterranean regions. More specifically, the WM data indicate generally higher coefficients of variations than the CRU data over most Mediterranean regions and in all seasons, particularly JJA. As mentioned, these differences can likely be attributed to the smoothing and interpolation procedure used to generate the gridded data.

Overall, both models show a generally good agreement with observations in DJF, MAM and SON, with a relatively small overestimation over the Iberian and Italian peninsulas in these seasons. In JJA, the RegCM shows greater coefficients of variation than HadAMH and the two observed datasets, particularly over the Mediterranean regions. A strong contribution to the higher summer precipitation variability in the RegCM compared to HadAMH is the scale effect identified by Giorgi (2002c), which is maximum for summer precipitation due to local convective processes. Over the Mediterranean regions another significant contribution to this difference in RegCM and HadAMH values is possibly due to the different coastline representations in the models, since differences in the behavior of convection over land and ocean are important in the summer.

Figure 9b shows that, in general, the correlation between (grid point) RegCM and HadAMH anomalies is lower for precipitation than for temperature, although some rather high values can be found in some western European regions (e.g., the British Isles, France and the Iberian peninsula). Over these regions evidently the precipitation interannual variability is mostly driven by the HadAMH simulation of the Atlantic storm track. As noted for temperature, JJA is also the season of minimum correlation for precipitation between HadAMH and RegCM interannual anomalies, an indication that in the summer the model simulation of local processes is most important in determining the precipitation variability. Note that only in a few cases does the boundary forcing explains more than half of the precipitation variability, even in the winter season. In fact, in JJA over the southeastern Mediterranean and Alpine regions the HadAMH/RegCM anomaly correlation coefficient is less than 0.3. These results indicate that, at the grid point level, the simulation of local and mesoscale processes and forcings (e.g., topography) contributes more than the large-scale lateral boundary forcing in determining the precipitation interannual variability.

In an analysis of large-scale precipitation interannual variability of CRU observations and HadCM3 simulations, Giorgi (2002a,b) found that the HadCM3 precipitation variability was generally in line with observations over the northern Europe region and it was overestimated over the Mediterranean region. These results are consistent with our analysis of the HadAMH variability and the RegCM variability as affected by HadAMH.

### 3.3 Trends

As mentioned in Sect. 1, it is useful to analyze the trends simulated by the models in relation to the observed trends for the period 1961–1990. This can in fact give some insights into the models ability to simulate regional climatic trends and changes in response to either external forcings or interdecadal modes of internal variability. A good performance in this regard can enhance the

confidence in the trends projected for future climate conditions.

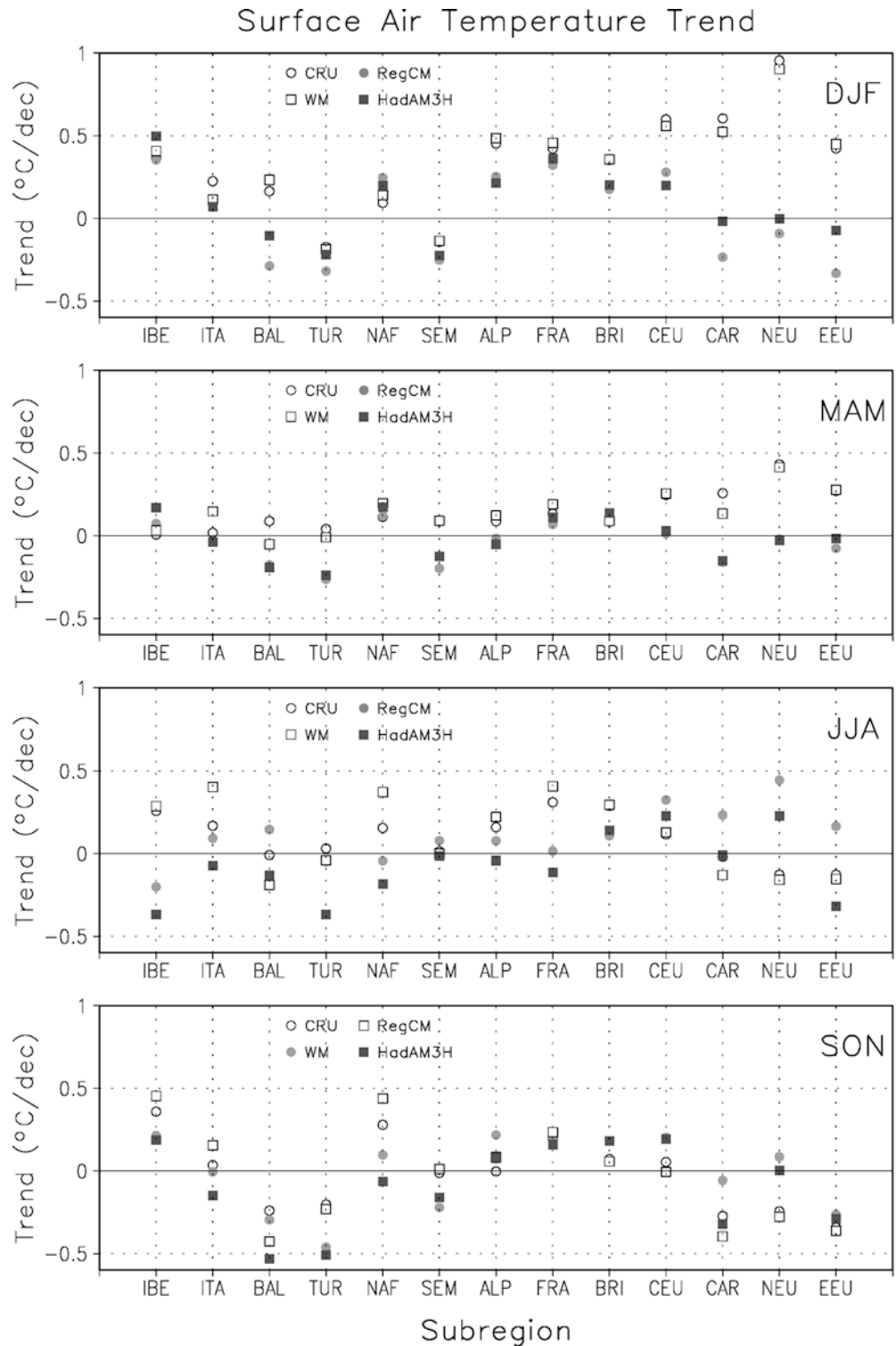
A limitation of the analysis presented in this section is that we only have available one realization of the reference period, and because all models are characterized by a certain level of internal variability, an ensemble of simulations is necessary to fully evaluate the model's ability to simulate trends for specific periods.

Nevertheless, because HadAMH utilizes observed SST fields and GHG forcing, it is reasonable to hypothesize that some regional climatic responses might be at least qualitatively captured for conditions in which these responses are strongly forced by SST anomalies or GHG forcing (Rodwell et al. 1999; Hoerling et al. 2001). Based on these considerations, our analysis of trends should mostly be considered as qualitative.

Figure 11 shows the observed (CRU and WM) and simulated (RegCM and HadAMH) surface air temperature linear trend values (in degrees per decade) during the period 1961–1990 averaged over the 13 regions of Fig. 1. To put these trends within a global context, we recall that the global temperature during this period did not show a strong trend except during the eighties, the largest warming of the late twentieth century having occurred in the nineties (e.g., Folland et al. 2001). Concerning the European region, the inter-decadal variability of European climate is strongly affected by the North Atlantic Oscillation (NAO) in the winter (e.g., Hurrell 1995). During the positive phase of the NAO, a ridge builds over Europe which causes a northward shift of the storm track and stronger and more southwesterly circulations over the continent (Hurrell 1995). This causes a general tendency towards warming of the European continental regions. Time series of the NAO index show that between 1961 and 1990 there was a marked trend of this index towards positive values, that is the NAO phase has become increasingly positive (Hurrell 1995). The observed positive winter temperature trends of Fig. 11 over the western and central European regions thus reflect this trend in the NAO phase.

For the other seasons, in general the effect of both the NAO and the El Niño Southern Oscillation (ENSO) on the variability of European climate is less important (e.g. Giorgi 2002a; Hurrell 1995; Philander 1990). The increase in GHG concentration could have a bigger effect but, as mentioned, at the global scale the 1961–1990 period did not show a pronounced warming, so it is difficult to identify a GHG signal. The observed trends may thus be the result of the combination of a number of factors, such as the forcing from SST, GHG and aerosol concentration, landuse change, volcanic and solar activity, or the result of the natural interdecadal variability of the climate system. What the observations indicate is that (1) in MAM the temperature trends are very small throughout western Europe and become positive in the northeastern European regions; and (2) both in JJA and SON the temperature trends are mostly positive over the western European regions and negative

**Fig. 11** Observed (CRU and WM) and simulated (RegCM and HadAMH) seasonal surface air temperature trend during the period 1961–1990 averaged over the 13 regions of Fig. 1. Only land data are included in the regional average. Units are degrees C/decade. Seasons are DJF, MAM, JJA and SON in order from the *top* to the *bottom* panel



over eastern European regions. The other important feature to note in Fig. 11 is that the trends in the two observed datasets are consistent with each other.

Similarities between observed and simulated temperature trends are found in SON over most regions and in DJF over the Mediterranean and western European regions. However, the models do not capture the winter

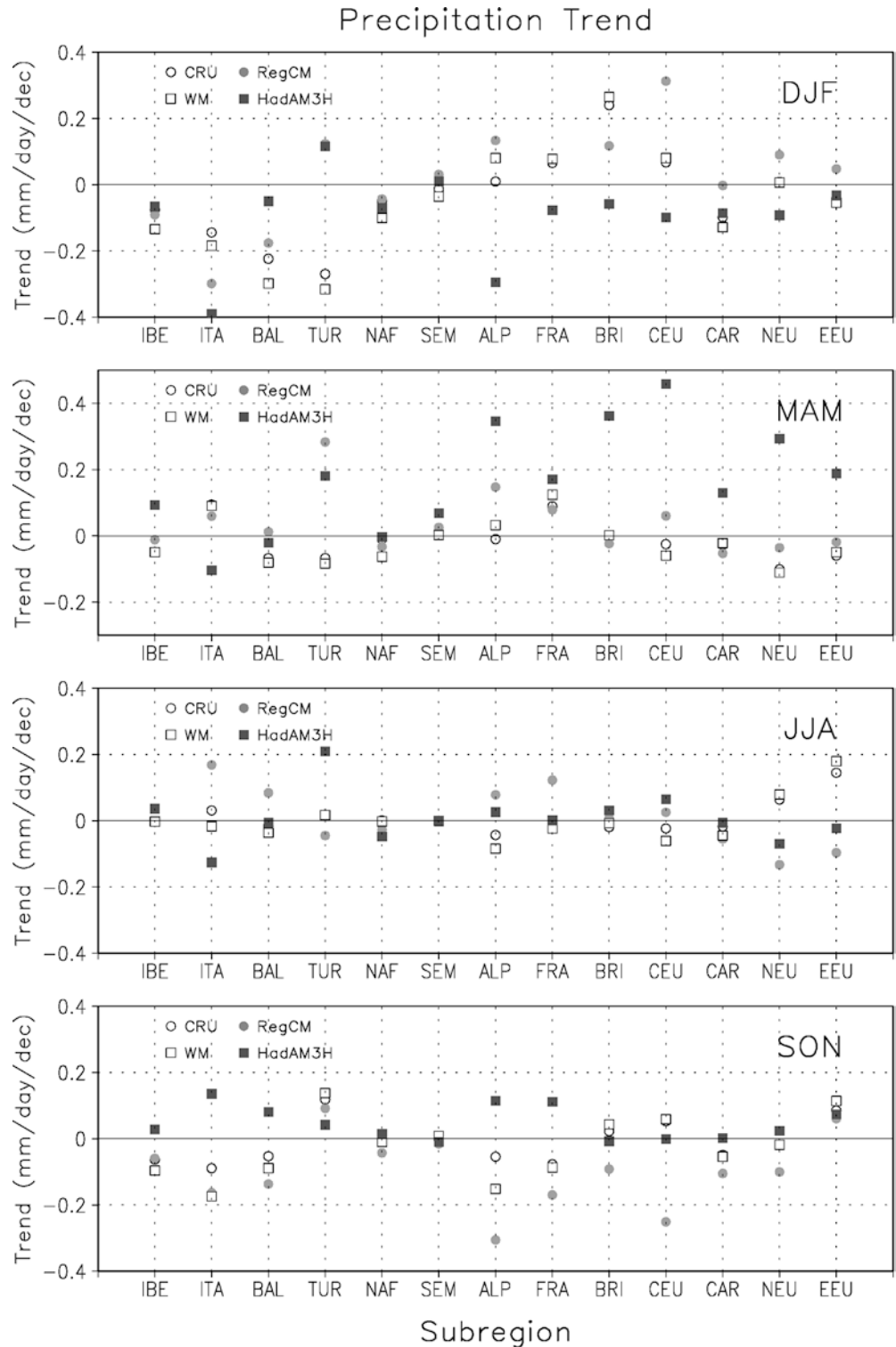
warming trend over the eastern European regions (CAR, NEU and EEU). In JJA and MAM, where the trends are relatively small, little agreement is found between simulations and observations. The RegCM and HadAMH trends are close to each other in DJF, SON and MAM, implying that they are essentially controlled by the HadAMH large-scale fields and boundary forcing.

Greater differences in magnitude are found in JJA, although the inter-regional pattern is still similar in the two models.

Observed and simulated regional precipitation trends for the period 1961–1990 are shown in Fig. 12. A noticeable feature of the observed DJF trend is the drying (negative trend) over the Mediterranean regions

(IBE, ITA, BAL, TUR) and the predominant positive precipitation trend over the western and central European regions. This trend signal has been again attributed to an increase in the positive phase of the NAO during 1961–1990, which produces a northward shift of the winter storm track over Europe resulting in reduced storm activity and precipitation over the Mediterranean

**Fig. 12** Observed (CRU and WM) and simulated (RegCM and HadAM3H) seasonal precipitation trend during the period 1961–1990 averaged over the 13 regions of Fig. 1. Only land data are included in the regional average. Units are mm/day/decade. Seasons are DJF, MAM, JJA and SON in order from the *top* to the *bottom* panel



region (Hurrell 1995). Predominantly negative observed precipitation trends in the Mediterranean regions, as well as over the Alps and France regions, are also found in SON. Conversely, in JJA the most prominent observed trend features are the positive trends over the NEU and EEU regions, while in MAM the observed precipitation trends are generally small.

Figure 12 indicates that a number of qualitative agreements between the observed and RegCM-simulated trends are found. In particular, in agreement with observations, in DJF the RegCM simulates drying over the Mediterranean regions (except over Turkey) and positive trends over the western and central European regions which, as mentioned, have been attributed to a trend in the NAO. Noticeable similarities in the observed and RegCM-simulated precipitation trends are also found over the Mediterranean, Alps and France regions in SON. Interestingly, Fig. 12 shows that a substantial disagreement in the trend simulation is found in a number of cases between the RegCM and HadAMH experiments, with the RegCM being generally closer to observations. Possibly, local feedbacks in the models can contribute significantly to the simulated trends in some of the subregions. For example, regional-scale interactions between soil moisture and precipitation can substantially affect regional precipitation patterns and trends (e.g., Pal and Eltahir 2003).

---

#### 4 Summary and discussion

We have analyzed means, interannual variability and trends in a 30-year simulation for the period 1961–1990 with the RegCM nested within a high resolution version of the Hadley Centre global atmospheric model HadAMH. Observed SST and GHG concentrations, along with sulfate aerosol fields calculated from HadAMH, are used in the simulations.

The first feature to note in our study is that the RegCM and HadAMH exhibit systematic differences in their surface climatology attributed, at least partially, to their different treatments of boundary layer and convective processes. The RegCM has a more efficient vertical transport of heat and water vapor, which results in significant differences of the vertical temperature and water vapor profiles compared to HadAMH and in mostly lower surface temperatures and higher precipitation amounts in the regional model. In some cases this is in the direction of greater agreement with observations, while in others it is in the opposite direction.

Overall, both the HadAMH and RegCM average climatologies are of good quality compared to previous experiments. Sub-regional seasonal temperature biases are generally less than 2°C and in many cases less than 1°C, while precipitation biases are mostly less than 10–20%, which is the level of uncertainty implied by the use of a gauge undercatch correction. Given that the subregions considered are of smaller size than in previous studies, these biases point to a general improvement of

nested GCM-RCM modeling systems over the European region. In this particular application, the RegCM shows a tendency to overestimate precipitation in MAM. This tendency was not noted in previous simulations using analyzes of observations as lateral boundary forcing, and therefore it is likely related to the model interaction with the HadAMH fields and in particular to the response of the RegCM to enhanced vertical transport of water vapor as discussed already. It is also important to emphasize that, as in previous simulations, the RegCM captures well the topography-induced surface climate signal at the resolution considered.

The models, and in particular the RegCM, show a prevailing tendency to overestimate interannual variability (except for DJF temperature), particularly during the summer and over the Mediterranean subregions. During the cold and intermediate seasons, the RegCM interannual variability is strongly regulated by the HadAMH forcing fields, especially for temperature. Scale effects however would tend to induce more pronounced variability in the RegCM than HadAMH (Giorgi 2002c). In summer, the RegCM interannual variability is less directly influenced by the HadAMH forcing, especially in the regions located in the domain interior and characterized by complex topographic and coastline features (e.g., the Mediterranean regions and the Alps). Giorgi (2002c) showed that the scale dependency of interannual variability is most pronounced in the summer, which is consistent with our results. Local and mesoscale land surface and convective processes, related for example to soil water feedbacks (Christensen et al. 2001), evidently play an important and perhaps dominant role in regulating the simulated interannual variability of warm season surface climate.

Note that in previous RegCM perfect boundary condition experiments (Giorgi and Shields 1999; Small et al. 1999; Sun et al. 1999; Pal et al. 2000) the model did not show a tendency to overestimate interannual variability. Therefore, the overestimate is again due to the model interaction with the HadAMH fields and possibly to the scale amplification effect discussed.

Despite the completion of a single realization, the HadAMH-RegCM modeling system captured a number of features of the observed surface climate trends during the 1961–1990 period over the European region, primarily for the cold seasons (DJF and SON). Most noticeably, the model captured the drying trend over the Mediterranean basin (except for the Turkish region) and the increasing precipitation trend over central Europe observed during the winter season, a feature attributed to the effect of the NAO during 1961–1990. Conversely, the model was not successful in reproducing the observed winter temperature trends over some eastern European regions. In this regard, we are currently carrying out a more detailed analysis of the NAO signal in the RegCM simulation to report in a separate study. With all the caveats implied by the use of a single realization, for which it cannot be ruled out that some of the agreements in the simulated and observed trends might

be fortuitous, our results provide encouraging indications towards the ability of climate models to simulate observed trends in response to observed forcings. However, given also that most trends were small and not statistically significant, ensembles of realizations are necessary to yield a more robust conclusion on this issue.

Our simulation included the direct and indirect (type I) effects of anthropogenic sulfate aerosols. It is difficult to rigorously evaluate the importance of aerosol effects in our experiment, since this would require the comparison with a corresponding aerosol-free simulation. However, previous RCM work, both with a different model over the European region (Ekman and Rodhe 2003) and our model over the east Asia region (Giorgi et al. 2002, 2003), indicate that sulfate aerosols can induce near-surface regional coolings in the range of several tenths of a degree to over one degree and can inhibit precipitation formation.

Overall, the reference simulation discussed confirms the trend towards increasingly good quality nested regional climate simulations, at least in mid-latitude regions. Higher resolution global models, such as HadAMH, appear capable of producing increasingly realistic large-scale forcing fields for nested RCMs and, from these, the RCMs are capable of producing realistic fine scale information as driven by fine scale processes and forcings (e.g., topography). In particular, the approach of using intermediate resolution time slice AGCM simulations to drive high resolution RCMs appears to be an especially promising one. We are in the process of analyzing higher frequency variability (e.g., daily) and extreme event statistics to further evaluate the model performance. The present reference simulation constitutes the basis to examine the climate change simulations resulting from the A2 and B2 forcing scenarios which will be reported in a separate study.

**Acknowledgements** This work was supported by the European Union Programme Energy, Environment and Sustainable Development under contract EVK2-2001-00156 (PRUDENCE). We would like to thank the Hadley Centre for providing the HadAMH data, the Climatic Research Unit for providing the CRU data and C. Willmott for providing the WM/LW data. We also thank two anonymous reviewers for their comments and suggestions, which helped to improve the quality of this work.

## References

- Adam JC, Lettenmaier DP (2003) Adjustment of global gridded precipitation for systematic bias. *J Geophys Res* 108: 4257 doi:10.1029/2002JD002499
- Christensen JH, Christensen OB (2003) Climate modelling: severe summertime flooding in Europe. *Nature* 421: 805–806
- Christensen JH, Machenhauer B, Jones RG, Schar C, Ruti PM, Castro M, Visconti G (1997) Validation of present-day regional climate simulations over Europe. LAM simulations with observed boundary conditions. *Clim Dyn* 13: 489–506
- Christensen JH, Carter TR, Giorgi F (2002) PRUDENCE employs new methods to assess European climate change. *EOS* 83: 147
- Christensen OB, Christensen JH, Machenhauer B, Bozet M (1998) Very-high resolution regional climate simulations over Scandinavia. Present climate. *J Clim* 11: 3204–3229
- Christensen OB, Gaertner MA, Prego JA, Polcher J (2001) Internal variability of regional climate models. *Clim Dyn* 17: 875–887
- Cocke S, LaRow TE (2000) Seasonal predictions using a regional spectral model embedded within a coupled ocean-atmosphere model. *Mon Weather Rev* 128: 689–708
- Cox PM, Betts RA, Bunton CB, Essery RLH, Rowntree PR, Smith J (1999) The impact of new land surface physics on the GCM simulation of climate and climate sensitivity. *Clim Dyn* 15: 183–203
- Cusack S, Edwards JM, Crowther JM (1999) Investigating k-distribution methods for parametrizing gaseous absorption in the Hadley Centre climate model. *J Geophys Res* 104: 2051–2057
- Dickinson RE, Henderson-Sellers A, Kennedy PJ (1993) Biosphere-Atmosphere Transfer Scheme (BATS) Version 1e as coupled to the NCAR Community Climate Model, NCAR Technical Note, NCAR/TN-387+STR, pp 72
- Edwards JM, Slingo A (1996) Studies with a flexible new radiation code. I: choosing a configuration for a large scale model. *Q J R Meteorol Soc* 122: 689–719
- Ekman AML, Rodhe H (2003) Regional temperature response due to indirect sulfate aerosol forcing: impact of model resolution. *Clim Dyn* 21: 1–10
- Fennessy MJ, Shukla J (2000) Seasonal prediction over North America with a regional model nested in a global model. *J Clim* 13: 2605–2627
- Folland CK, Karl TL, Christy JR, Clarke RA, Gruza GV, Jouzel J, Mann ME, Oerlemans J, Salinger MJ, Wang S-W (2001) Observed climate variability and change. In: Houghton JT, Ding Y, Griggs DJ, Noguer M, van der Linden PJ, Xiaoxu D (eds) Chapter 2 of Climate change 2001; The scientific basis. Contribution of Working Group I to the Third Assessment Report of the Intergovernmental Panel on Climate Change (IPCC), Cambridge University Press, Cambridge, UK, pp 99–181
- Fukutome S, Frei C, Luthi D, Schar C (1999) The interannual variability as a test ground for regional climate simulations over Japan. *J Meteorol Soc Japan* 77: 649–672
- Giorgi F (2002a) Variability and trends of sub-continental scale surface climate in the twentieth century. Part I: Observations. *Clim Dyn* 18: 675–691
- Giorgi F (2002b) Variability and trends of sub-continental scale surface climate in the twentieth century. Part II: AOGCM simulations. *Clim Dyn* 18: 693–708
- Giorgi F (2002c) Dependence of surface climate interannual variability on spatial scale. *Geophys Res Lett* 29: 2101, doi: 10.1029/2002GL016175
- Giorgi F, Mearns LO (1991) Approaches to regional climate change simulation: a review. *Rev Geo* 29: 191–216
- Giorgi F, Marinucci MR (1996a) An investigation of the sensitivity of simulated precipitation to model resolution and its implications for climate studies. *Mon Weather Rev* 124: 148–166
- Giorgi F, Marinucci MR (1996b) Improvements in the simulation of surface climatology over the European region with a nested modeling system. *Geophys Res Lett* 23: 273–276
- Giorgi F, Mearns LO (1999) Introduction to special section: regional climate modeling revisited. *J Geophys Res* 104: 6,335–6,352
- Giorgi F, Shields C (1999) Tests of precipitation parametrizations available in the latest version of the near regional climate model (RegCM) over continental US. *J Geophys Res* 104: 6,353–6,375
- Giorgi F, Marinucci MR, Visconti G (1992) A 2XCO<sub>2</sub> climate change scenario over Europe generated using a limited area model nested in a general circulation model II: climate change scenario. *J Geophys Res* 97: 1,0011–1,0028
- Giorgi F, Marinucci MR, Bates GT (1993a) Development of a second generation regional climate model (RegCM2). Part I. Boundary-layer and radiative transfer processes. *Mon Weather Rev* 121: 2,794–2,813
- Giorgi F, Marinucci MR, Bates GT, De Canio G (1993b) Development of a second generation regional climate model (RegCM2). Part II. Convective processes and assimilation of lateral boundary conditions. *Mon Weather Rev* 121: 2,814–2,832

- Giorgi F, Hurrell JW, Marinucci MR, Beniston M (1997) Elevation signal in surface climate change: a model study. *J Clim* 10: 288–296
- Giorgi F, Hewitson B, Christensen JH, Hulme M, vonStorch H, Whetton P, Jones R, Mearns LO, Fu C (2001) Regional Climate Information - Evaluation and Projections. In: Houghton JT, Ding Y, Griggs DJ, Noguer M, van der Linden PJ, Xiaoxu D (eds) Chapter 10 of climate change 2001; the scientific basis. Contribution of Working Group I to the Third Assessment Report of the Intergovernmental Panel on Climate Change (IPCC), Cambridge University Press, Cambridge, UK, pp 583–638
- Giorgi F, Bi X, Qian Y (2002) Direct radiative forcing and regional climatic effects of anthropogenic aerosols over east Asia: a regional coupled climate-chemistry/aerosol model study. *J Geophys Res* 107: Art No 4439, doi:10.1029/2001JD001066
- Giorgi F, Bi X, Qian Y (2003) Indirect versus direct effects of anthropogenic sulfate on the climate of east Asia as simulated with a regional coupled climate-chemistry/aerosol model. *Clim Change* 58: 345–376
- Gregory D, Rowntree PR (1990) A mass flux convection scheme with representation of cloud ensemble characteristics and stability dependent closure. *Mon Weather Rev* 118: 1483–1506
- Gregory D, Allen S (1991) the effect of convective scale downdrafts upon NWP and climate simulations. Ninth Conf Numerical Weather Prediction. Denver, Colorado, American Meteorological Society, pp 122–123
- Gregory D, Morris D (1996) The sensitivity of climate simulations to the specification of mixed phase clouds. *Clim Dyn* 12: 641–651
- Grell GA (1993) Prognostic evaluation of assumptions used by cumulus parameterizations. *Mon Weather Re* 121: 764–787
- Grell GA, Dudhia J, Stauffer DR (1994) A description of the fifth generation Penn State/NCAR Mesoscale Model (MM5). NCAR Technical Note, NCAR/TN-398 + STR, pp 121
- Hoerling MP, Hurrell JW, Xu T (2001) Tropical origins for recent North Atlantic climate change. *Science* 292: 90–92
- Holtzlag AAM, de Bruijn EIF, Pan HL (1990) A high resolution air mass transformation model for short-range weather forecasting. *Mon Weather Re* 118: 1561–1575
- Hurrell JW (1995) Decadal trends in the North Atlantic Oscillation regional temperatures and precipitation. *Science* 269: 676–679
- IPCC (1998) The regional impacts of climate change, an assessment of vulnerability, Watson RT, Zinyowera MC, Moss RH, Dokken DJ (eds) Cambridge University Press, Cambridge, UK, pp 517
- IPCC (2000) Emission scenarios, In: Nakicenovic N (ed) A special report of Working Group III of the Intergovernmental Panel on Climate Change, Cambridge University Press, Cambridge, UK, pp 599
- IPCC (2001) Climate change 2001; The scientific basis, In: Houghton JT, Ding Y, Griggs DJ, Noguer M, van der Linden PJ, Xiaoxu D (eds) Contribution of Working Group I to the Third Assessment Report of the Intergovernmental Panel on Climate Change (IPCC), Cambridge University Press, Cambridge, UK, pp 583–638
- Ji YM, Vernekar AD (1997) Simulation of the Asian summer monsoons of 1987 and 1988 with a regional model nested in a global GCM. *J Clim* 10: 1965–1979
- Johns TC, Gregory JM, Ingram WJ, Johnson CE, Jones A, Mitchell JFB, Roberts DL, Sexton DMH, Stevenson DS, Tett SFB, Woodage MJ (2001) Anthropogenic climate change for 1860 to 2100 simulated with the HadCM3 model under updated emission scenarios. Hadley Centre Technical Note 22 pp 62
- Jones RG, Murphy JM, Noguer M (1995) Simulation of climate change over Europe using a nested regional climate model. I: assessment of control climate, including sensitivity to location of lateral boundary conditions. *Q J R Meteorol Soc* 121: 1413–1449
- Jones RG, Murphy JM, Noguer M, Keen M (1997) Simulation of climate change over Europe using a nested regional climate model. I: Comparison of driving and regional model responses to a doubling of carbon dioxide. *Q J R Meteorol Soc*. 123: 265–292
- Kalnay M, Kanamitsu M, Kistler R, Collins W, Deaven D, Gandin L, Iredell M, Saha S, White G, Woollen J, Zhu Y, Chelliah M, Ebisuzaki W, Higgins W, Janowiak J, Mo KC, Ropelewski C, Wang J, Leetma A, Reynolds R, Jjamme R, Joseph D (1996) The NCEP/NCAR 40-year reanalysis project. *Bull Am Meteorol Soc* 77: 437–471
- Kiehl JT, Hack JJ, Bonan GB, Boville BA, Briegleb BP, Williamson DL, Rasch PJ (1996) Description of the NCAR Community Climate Model (CCM3). NCAR Technical Note, NCAR/TN-420 + STR, pp 152
- Lal M, Bhaskaran B, Singh SK (1998) Indian summer monsoon variability as simulated by a regional model nested in a global model. *Chinese J Atmos Sci* 22: 93–102
- Legates DR, Willmott CJ (1990) Mean seasonal and spatial variability in gauge-corrected global precipitation. *Int J Climatol* 10: 111–127
- Loveland TR, Merchant JW, Ohlen DO, Brown JF (1991) Development of a land cover characteristics database for the conterminous United States. *Photogrammetric Eng Rem Sens* 57: 1453–1463
- Luthi D, Cress A, Davies XC, Frei C, Schar C (1996) Interannual variability and regional climate simulations. *Theor Appl Climatol* 53: 185–209
- Machenhauer B, Windelband M, Botzet M, Christensen JH, Deque M, Jones RG, Ruti PM, Visconti G (1998) Validation and analysis of regional present-day climate and climate change simulations over Europe. MPI Report 275, MPI, Hamburg, Germany
- Marinucci MR, Giorgi F (1992) A 2XCO<sub>2</sub> climate change scenario over Europe generated using a limited area model nested in a general circulation model I. Present day climate simulation. *J Geophys Res* 97: 9,989–10,009
- McGregor JJ (1997) Regional climate modelling. *Meteorol Atmos Phys* 63: 105–117
- New MG, Hulme M, Jones PD (1999) Representing twentieth-century space time climate variability. Part I. Development of a 1961–1990 mean monthly terrestrial climatology. *J Clim* 12: 829–856
- New MG, Hulme M, Jones PD (2000) Representing twentieth-century space time climate fields. Part II. Development of a 1901–1996 mean monthly terrestrial climatology. *J Clim*. 13: 2217–2238
- Pal JS, Eltahir EAB (2003) A feedback mechanism between soil moisture distribution and storm tracks. *Q J R Meteorol Soc* 129: 2,279–2,298
- Pal JS, Small EE, Eltahir EAB (2000) Simulation of regional - scale water and energy budgets: representation of subgrid cloud and precipitation processes within RegCM. *J Geophys Res* 105: 29,579–29,594
- Philander SGH (1990) El Nino, La Nina and the Southern Oscillation. Academic Press, New York, pp 293
- Pope VD, Gallani ML, Rowntree PR, Stratton RA (2000) The impact of new physical parametrizations in the Hadley Centre Climate model. *Clim Dyn* 16: 123–146
- Räisänen J, Joëlsson R (2001) Changes of average and extreme precipitation in two regional climate model experiments. *Tellus A* 53: 547–566
- Räisänen J, Rummukainen M, Ullerstig A (2001) Downscaling of greenhouse gas induced climate change in two GCMs with the Rossby Centre regional climate model for Northern Europe. *Tellus A* 53: 168–191
- Rayner NA, Parker DE, Horton EB, Folland CK, Alexander LV, Rowell DP, Kent EC, Kaplan A (2003) Global analyses of SST, sea ice, and night marine air temperature since the late nineteenth century. *J Geophys Res* 108: 4407, doi: 10.1029/2002JD002670
- Rodwell MJ, Rowell DP, Folland CK (1999) Oceanic forcing of the wintertime North Atlantic Oscillation and European climate. *Nature* 398: 320–323
- Rojas M, Seth A (2003) Simulation and sensitivity in a nested modeling system for South America. Part II: GCM boundary forcing. *J Clim* 16: 2454–2471

- Rotach MW, Marinucci MR, Wild M, Tschuck P, Ohmura A, Beniston M (1997) Nested regional simulation of climate change over the Alps for the scenario of a doubled greenhouse forcing. *Theor Appl Climatol* 57: 209–227
- Seth A, Rojas M (2003) Simulation and sensitivity in a nested modeling system for South America. Part I. Reanalysis boundary forcing. *J Clim* 16: 2437–2453
- Small EE, Giorgi F, Sloan LC (1999) Regional climate model simulation of precipitation in central Asia: mean and interannual variability. *J Geophys Res* 104: 6563–6582
- Smith RNB (1990) A scheme for predicting layer clouds and their water content in a general circulation model. *Q J R Meteorol Soc* 116: 435–460
- Smith RNB (1993) Experience and developments with the layer cloud and boundary layer mixing schemes in the UK Meteorological Office Unified Model. In: Proc ECMWF/GCSS workshop on parametrization of the cloud-topped boundary layer, 8–11 June 1993, ECMWF, Reading, UK
- Sun L, Semazzi FHM, Giorgi F, Ogallo L (1999) Application of the NCAR regional climate model to eastern Africa. Part II. Simulation of interannual variability of short rains. *J Geophys Res* 104: 6549–6562
- Willmott CJ, Matsuura K (2001) Terrestrial air temperature and precipitation: monthly and annual time series (1950–1999) (version 1.02). Center for Climate Research University of Delaware Newark, N.J., USA